



International Workshop on Advances in Laboratory Testing of Liquefiable Soils



The use of binders to avoid tailings' liquefaction

Nilo Cesar Consoli, Ph.D., P.Eng.

Professor of Civil Engineering - Department of Civil Engineering
Universidade Federal do Rio Grande do Sul - BRAZIL

E-mail: consoli@ufrgs.br

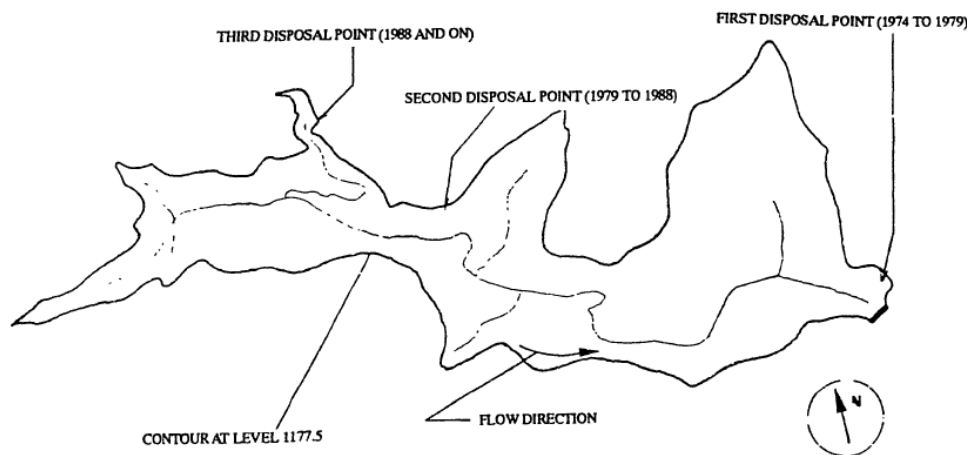
224 peer reviewed journal papers at Web of Science with 5936 citations and *h-index* = 44

Soil formation in a tailings' reservoir

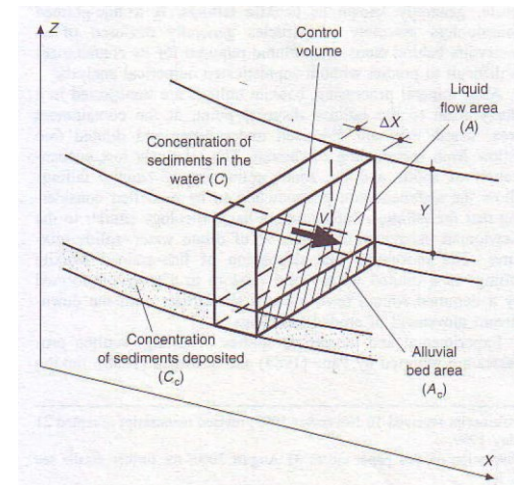
Soil formation from tailings disposed behind dams

3D modelling of the whole process of tailings disposal through spigotting, transport of sediments, sedimentation and consolidation simulating soil formation **behind dams**

This study was carried out in order to **produce a tool to establish the mass of tailings to be stored in the reservoir**



Plan view, flow direction and spigot disposal points of the analysed reservoir



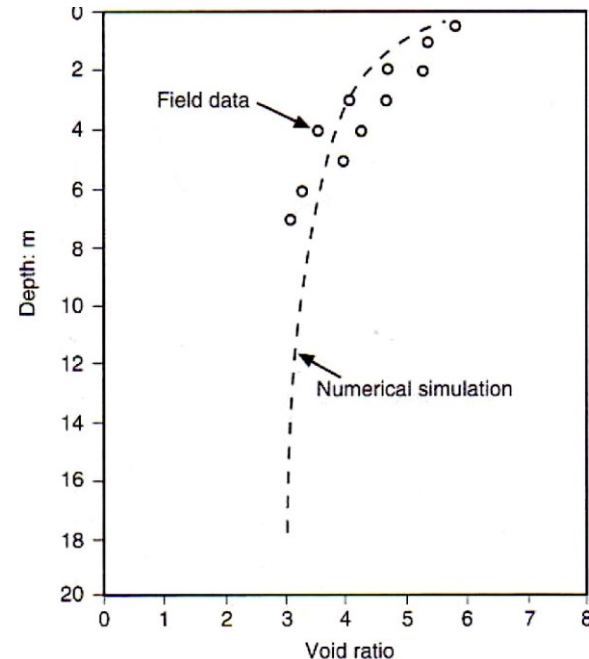
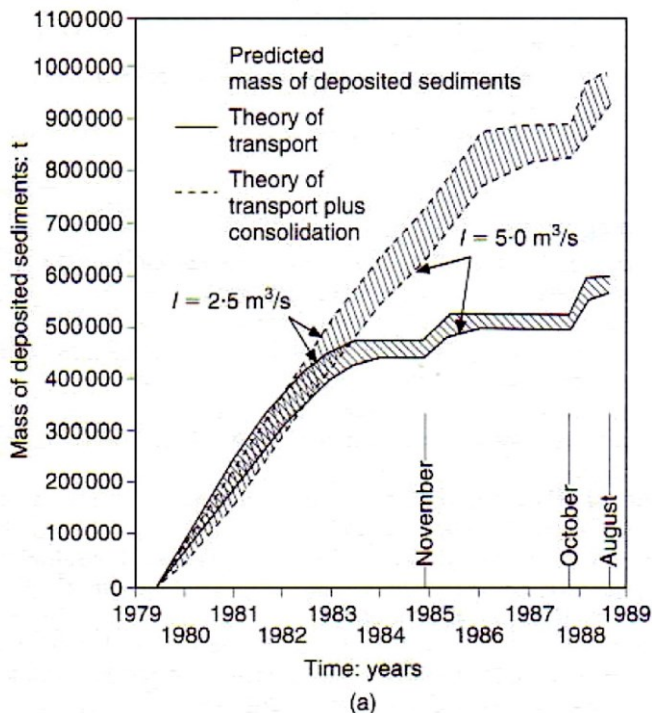
Schematic of stream

Telford Prize (2001) by Institution of Civil Engineers - UK



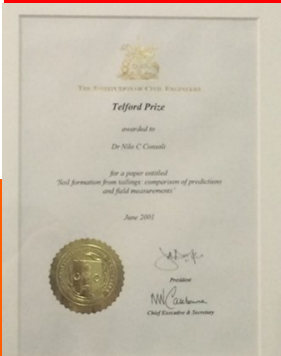
Consoli, N.C.; Sills, G. C. (2000)
“Soil formation from tailings: Comparison of predictions and field measurements”
Géotechnique, ICE/UK, v. 50, n.1, p. 25-33

Soil formation from tailings disposed behind dams



This study was carried out in order to produce a tool to establish the mass of tailings to be stored in the reservoir.

Telford Prize (2001) by Institution of Civil Engineers - UK



Consoli, N.C.; Sills, G. C. (2000)
"Soil formation from tailings: Comparison of predictions and field measurements"
Géotechnique, ICE/UK, v. 50, n.1, p. 25-33

Brumadinho upstream tailings dam failure (Brazil)



**Particle breakage
associated to field
compaction of filtered
ore tailings for dry
stacking**

Filtered tailings improvement through Compaction

When somebody is talking about mechanical behaviour of filtered tailings under high confining stresses, ones is talking about alternative ways of disposing ore tailings by stacking up to 300 meters (or even more) in a safe way, avoiding any possibility of liquefaction/failure.

For doing so, there is a knowledge acquired regarding ground improvement that can help in looking for possible solutions. Looking at the field, the first and most popular improvement technique is soil/filtered tailings compaction.



22 tonnes vibratory roller compactor
(to compact layers of up to about 50 cm)



Towed 22 tonnes three-sided impact compactor roller (effective to 2-4 m depth)

Another point to be noted is that the production of ore tailings might be in the order of 50,000-100,000 tonnes per day in a unique place, needing to think about alternatives to compacting layers of about 30-50 cm with standard compaction equipment, by using impact compactor rollers.

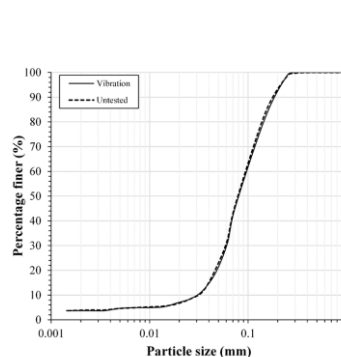
Particle breakage associated to field compaction of filtered iron ore tailings for dry stacking

Tailings dry stack are compacted in layers from the use of drum rollers that causes compaction and vibration efforts on the ground. Particle breakage is usually observed in granular materials when subjected to external loads as occurs with the increase of the dry stack height. However, the particle breakage also may occur during the layers' compaction. An iron ore tailings (53.60% fine sand, 39.90% silt, 6.40% clay size presenting 78.4% of quartz and 17.2% of iron oxide) classified as silty sand (SM) was subject to cyclic oedometer, compaction (Proctor at standard and modified effort), and vibration (determination of maximum index density) tests. Particle size distribution analyses were performed before and after testing all specimens.

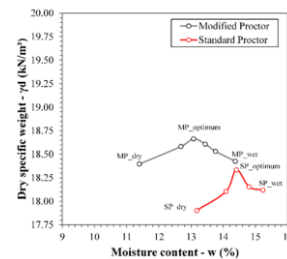
The influence of vibration on particle breakage was evaluated considering the recommendations of ASTM D4253. This standard presents test methods for the determination of the maximum index density of cohesionless soils using a vertically vibrating table.

The compaction characteristics of the tailings studied were assessed under standard and modified efforts following the recommendations of ASTM D698 and ASTM D1557, respectively

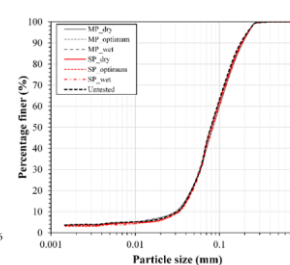
Cyclic oedometer tests were used to simulate the compaction of both tailings with drum rollers at field. Three pressures defined (1.9, 12.5, and 83.3 MPa) and considering the 100 mm sample diameter, the axial forces chosen for oedometer tests were 15, 100, and 700 kN respectively. Similar to the roller compaction, a loading frequency of 35 Hz was chosen, in addition to a lower frequency (10 Hz) to evaluate this influence. Also, 100, 1000, and 10000 cycles were adopted in the loadings to simulate different numbers of passes of the roller .



PSD after e_{min} tests



PSD after compaction tests



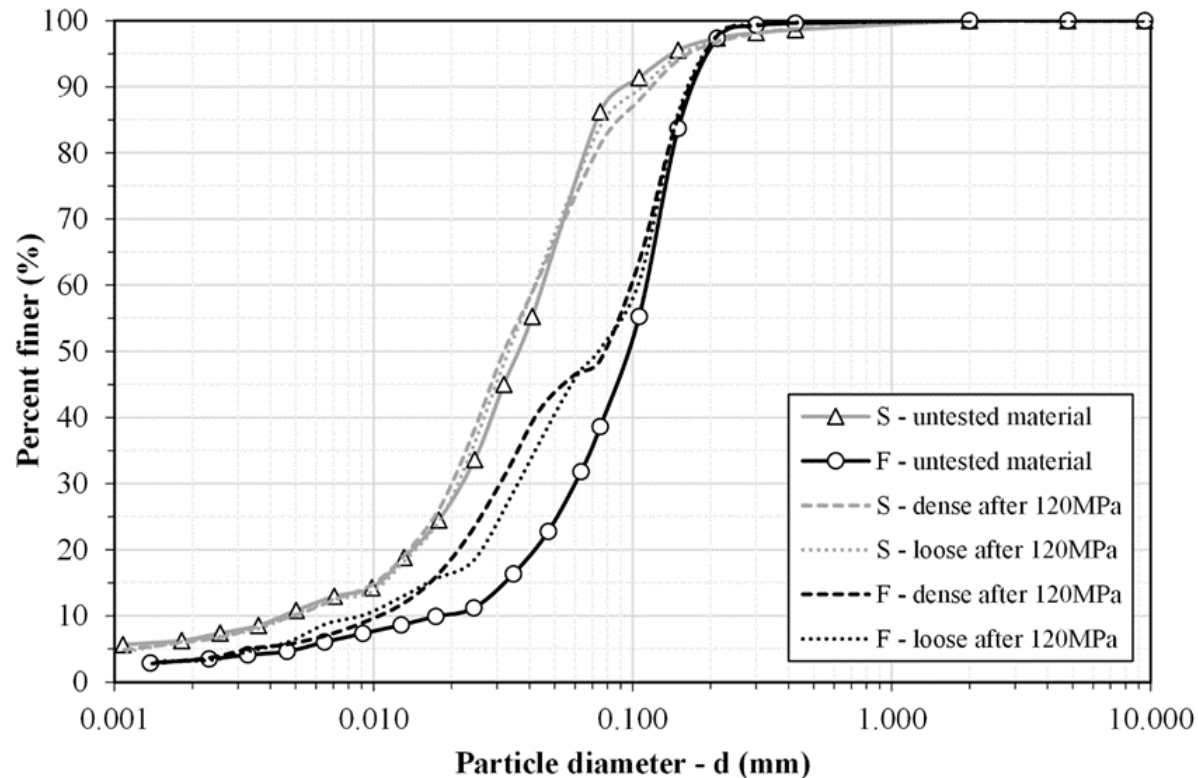
PSD after tests on cyclic oedometer equipment

Consoli, N.C. et al. (2022).

“On the particle breakage associated to field compaction of iron ore tailings for dry stacking.” *Géotechnique Letters*, ICE/UK (to be submitted for publication)

**Particle breakage
associated to high
pressures (due to filtered
compacted tailings dry
stacking)**

Tailings particle breakage when submitted to high pressures due to dry stack



Particle size distribution of two distinct gradings of untested and tested ore tailings.

**Main option studied in
Brazil to substitute
upstream tailings dam:
Filtered compacted dry
stacking (300 m high)**

Influence of Grading and Fabric Arising from the Initial Compaction on the Geomechanical Characterisation of Compacted Copper Tailings



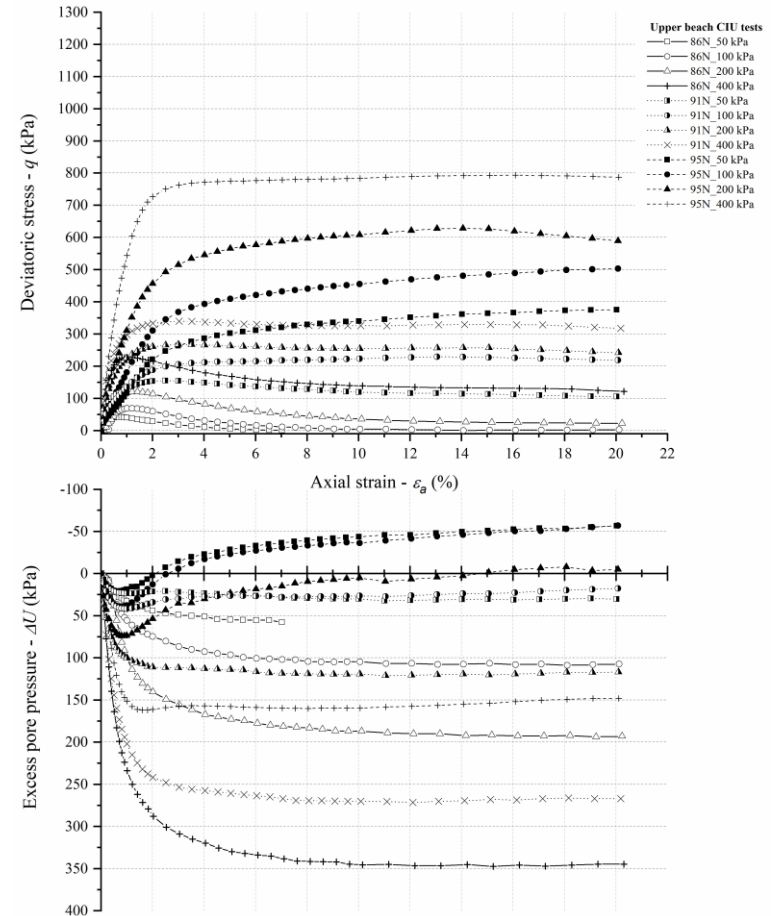
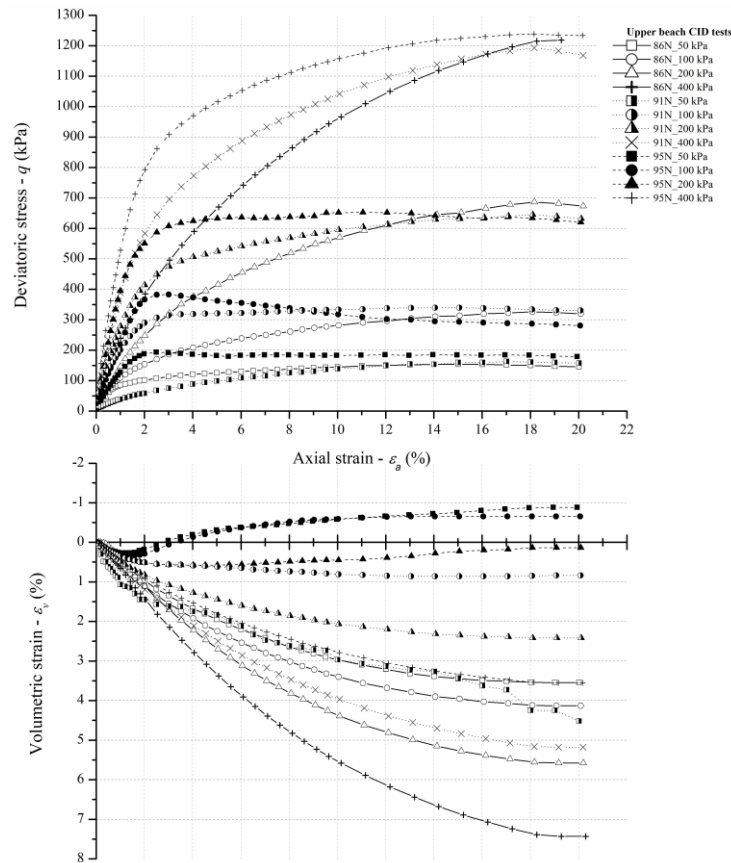
Copper tailings' collection points.

Influence of Grading and Fabric Arising from the Initial Compaction on the Geomechanical Characterisation of Compacted Copper Tailings

| Parameters | Samples | |
|-----------------------------------------------------------------------------|-------------|-------------|
| | upper beach | lower beach |
| Specific gravity – G_s | 2.844 | 2.943 |
| Gravel (%) | 0 | 0 |
| Coarse sand (%) | 1.5 | 0 |
| Medium sand (%) | 61.0 | 20.0 |
| Fine sand (%) | 25.0 | 54.5 |
| Silt (%) | 10.5 | 22.5 |
| Clay (%) | 2.0 | 3.0 |
| LL (%) | - | - |
| IP (%) | Non-plastic | Non-plastic |
| ASTM-USCS Classification | SM | SM |
| Maximum void ratio – e_{max} | 1.050 | 1.127 |
| Minimum void ratio – e_{min} | 0.831 | 0.842 |
| Standard Proctor optimum moisture content – w_{opt} (%) | 3.12 | 5.43 |
| Standard Proctor maximum dry density – γ_{dmax} (kN/m ³) | 16.68 | 17.26 |

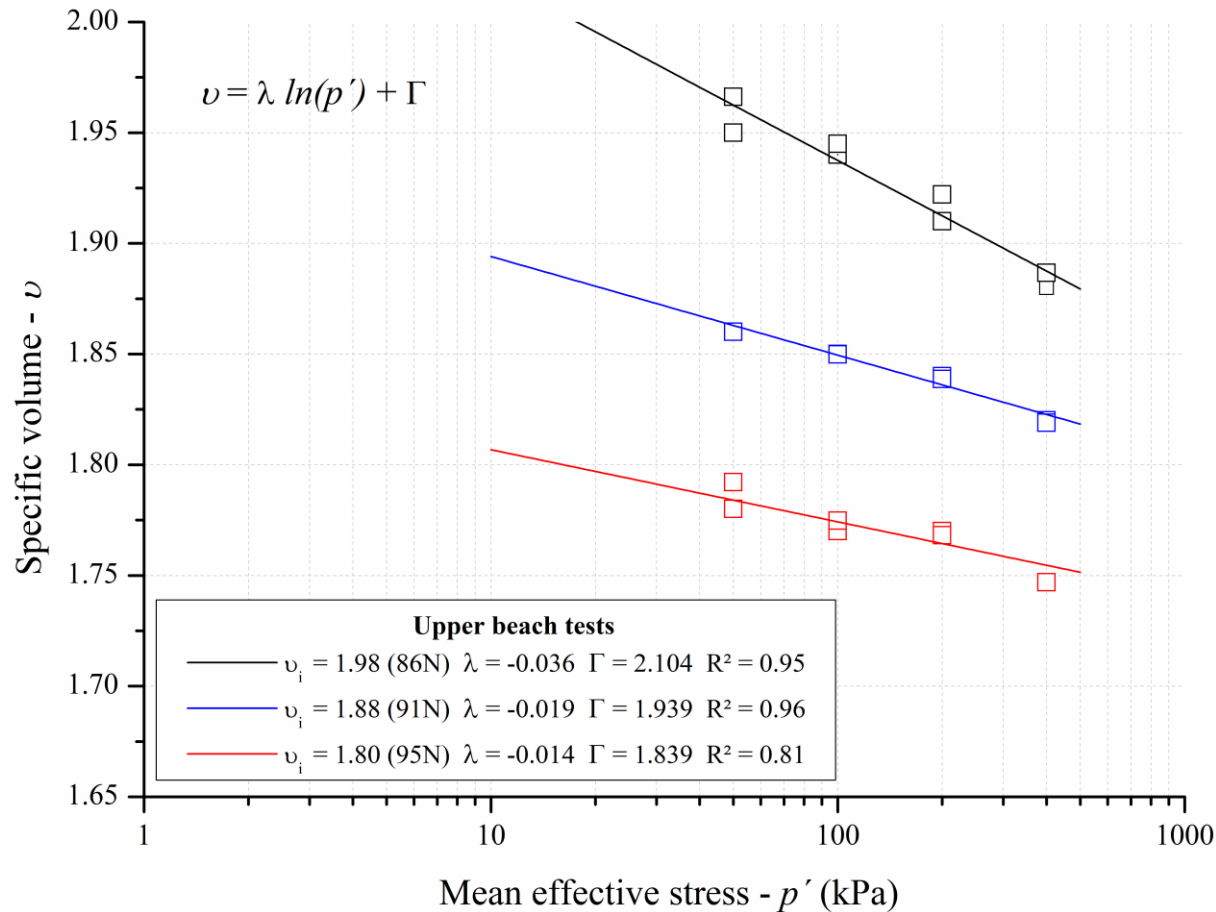
Physical properties of copper tailings.

Influence of Grading and Fabric Arising from the Initial Compaction on the Geomechanical Characterisation of Compacted Copper Tailings



Triaxial tests outcomes from specimens moulded using samples of the upper beach tailings: CID tests & CIU tests.

Influence of Grading and Fabric Arising from the Initial Compaction on the Geomechanical Characterisation of Compacted Copper Tailings



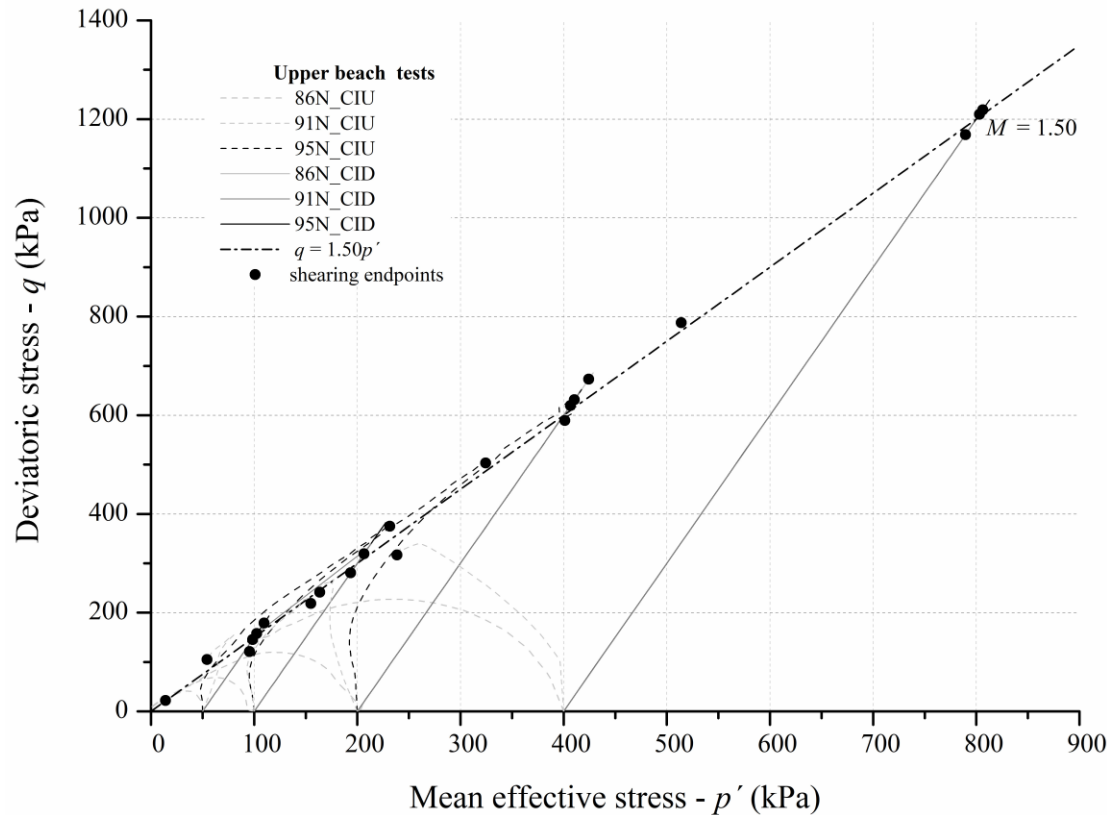
Isotropic compression data of the upper beach tailings.

Velten, R.Z.; Consoli, N.C. et al. (2022).

“Influence of grading and fabric arising from the initial compaction on the geomechanical characterisation of compacted copper tailings.”

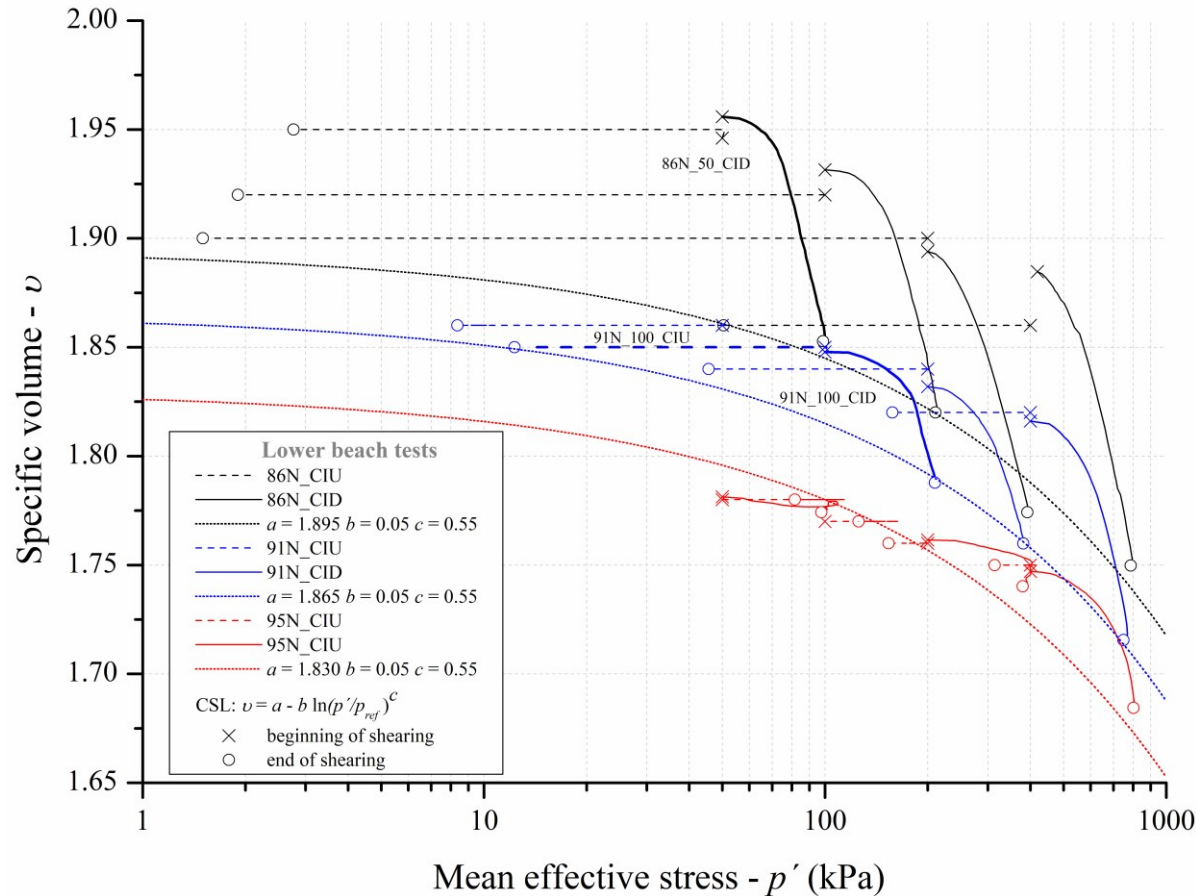
Géotechnique (accepted for publication).

Influence of Grading and Fabric Arising from the Initial Compaction on the Geomechanical Characterisation of Compacted Copper Tailings



Stress paths and critical state lines in the $q - p'$ space for samples of the upper beach tailings.

Influence of Grading and Fabric Arising from the Initial Compaction on the Geomechanical Characterisation of Compacted Copper Tailings



Critical state lines in the $v - \log p'$ space for samples of the lower beach tailings.

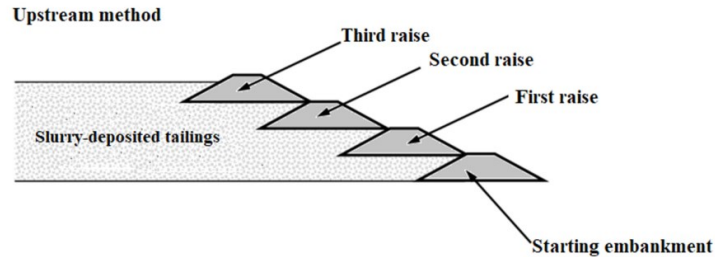
Velten, R.Z.; Consoli, N.C.; et al. (2022).

“Influence of grading and fabric arising from the initial compaction on the geomechanical characterisation of compacted copper tailings.”

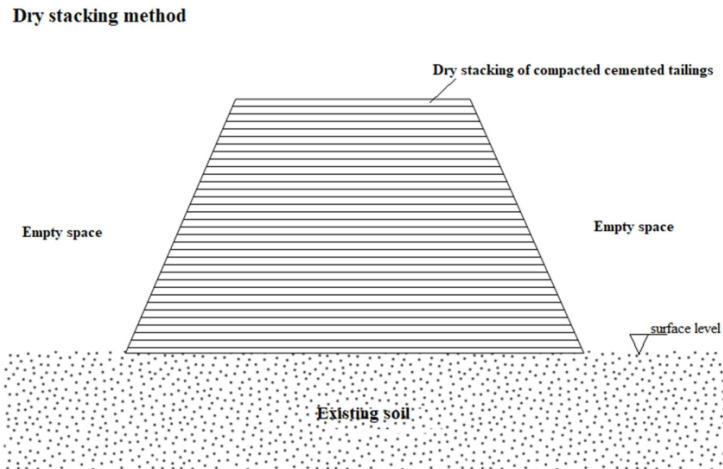
Géotechnique (accepted for publication).

**Another option studied
in Brazil to substitute
tailings dam:
Filtered compacted
cemented dry stacking
(300 m high)**

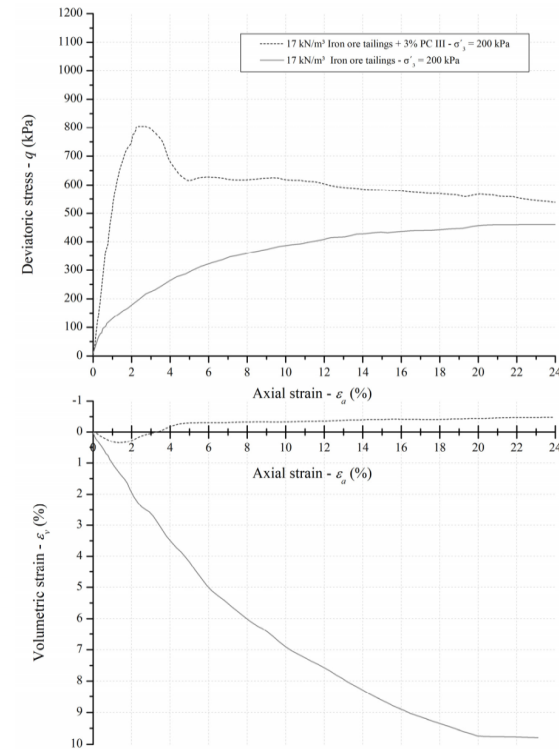
Dry Stacking Compacted Cemented Tailings



(a)



(b)



POROSITY/BINDER INDEX

Paradigm break: porosity/binder index

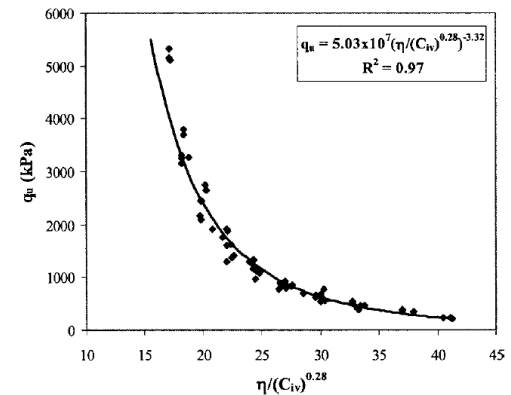
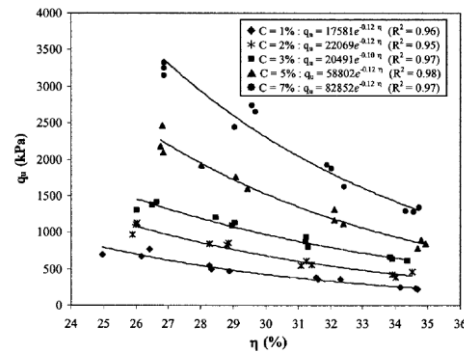
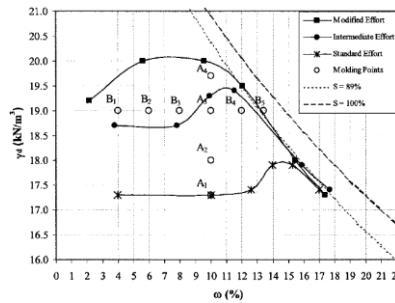
Consoli et al.(2007) developed a rational methodology that considers both the porosity and the quantity of cement through the index η/C_{iv} . This ratio is between the porosity of the compacted mixture (η) and the volumetric cement content (C_{iv}) that is added to the mixture

$$\frac{\eta}{C_{iv}} = \frac{\frac{V_v}{V_{total}}}{\frac{V_c}{V_{total}}} = \frac{V_v}{V_c}$$

where V_v = volume of voids (water + air) of the specimen;
 V_c = volume of cement of the specimen; and V_{total} = total volume of the specimen.

POROSITY/BINDER INDEX

Paradigm break: porosity/binder index
controls the unconfined compressive strength



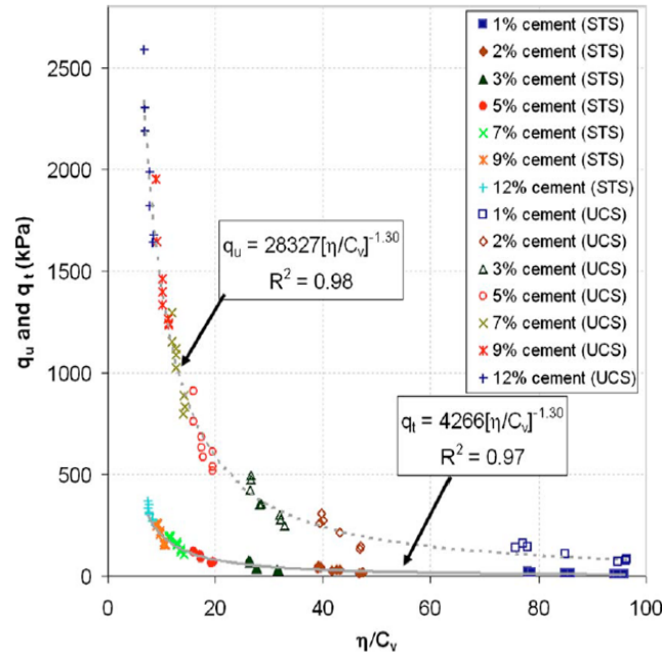
POROSITY/BINDER INDEX

Theoretical derivation of the porosity/binder index controlling the unconfined compressive strength

Diambra et al. (2017) established a theoretical derivation of the porosity/binder index. Knowing that the artificially cemented soil composite material is composed of the soil phase (the granular matrix) and the cement phase, assuming isotropy of the material, behavior of the cemented soil at the failure point being determined by superposing the strength contributions of both phases, failure of the composite cemented material occurs as a result of a simultaneous failure of both the cemented and soil matrix phases, strain compatibility between the composite and its two phases and defining the state parameter in terms of the material porosity (η), the following equation was derived:

$$q_u = \frac{6M\sigma_c^c(-0.6 + 0.45K_c)\eta_{cs}^a}{100[K_c(1 - \beta) + 3(\beta + 1)]} \left(\frac{\eta}{C_{iv}^{1/a}} \right)^{-a} = B \left(\frac{\eta}{C_{iv}^{1/a}} \right)^{-a}$$

POROSITY/BINDER INDEX



Variation of both splitting tensile (q_t) and unconfined compressive strengths (q_u) with voids/cement ratio

Porosity/cement ratio (η/C_{iv})

[controls not only the unconfined compressive strength, but also tensile strength, triaxial failure envelope, stiffness (G_o , B_o) amongst other mechanical properties]

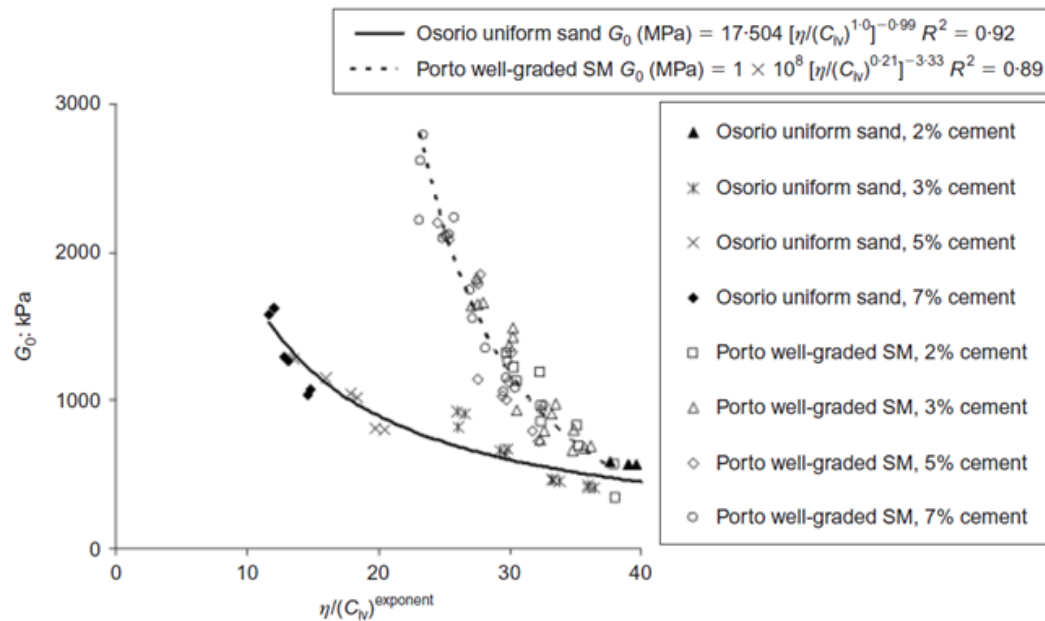
$$\frac{q_t}{q_u} = \frac{4,266 \left[\frac{\eta}{C_v} \right]^{-1.30}}{28,327 \left[\frac{\eta}{C_v} \right]^{-1.30}} = 0.15$$

Consoli, N.C.; Cruz, R.C.; Floss, M.F.; Festugato, L. (2010)

“Parameters controlling tensile and compressive strength of artificially cemented sand”

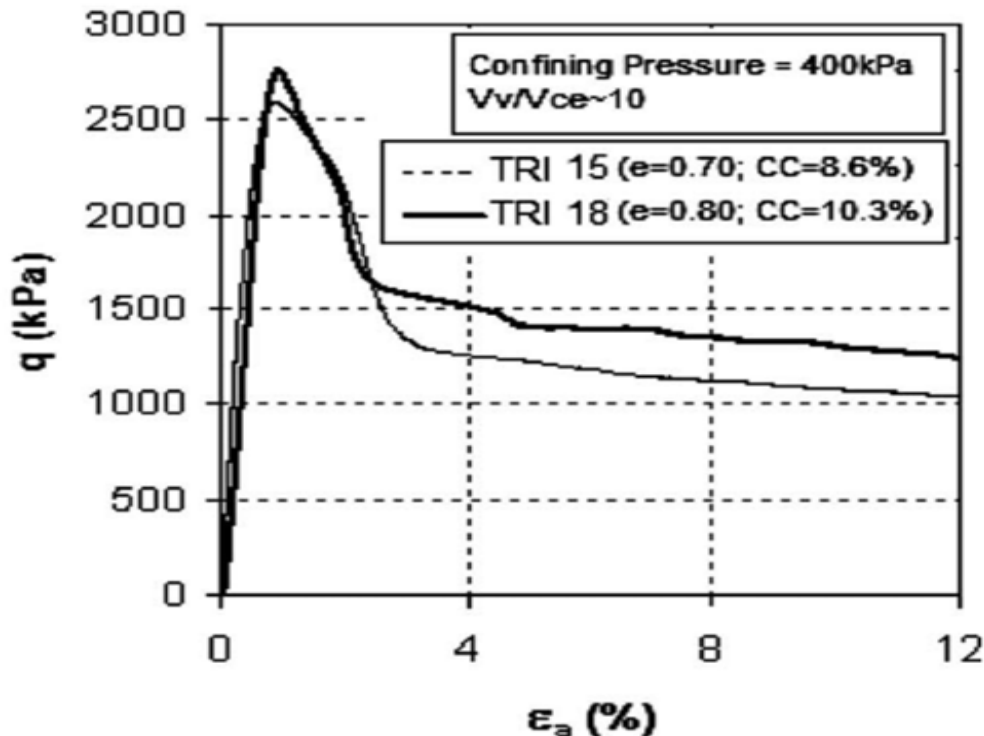
Journal of Geotechnical and Geoenvironmental Engineering, v. 136, p. 759-763

POROSITY/BINDER INDEX



Variation of initial shear modulus G_0 for both cemented soils (uniform sand and very well-graded silty sand) with adjusted porosity/cement ratio

POROSITY/BINDER INDEX

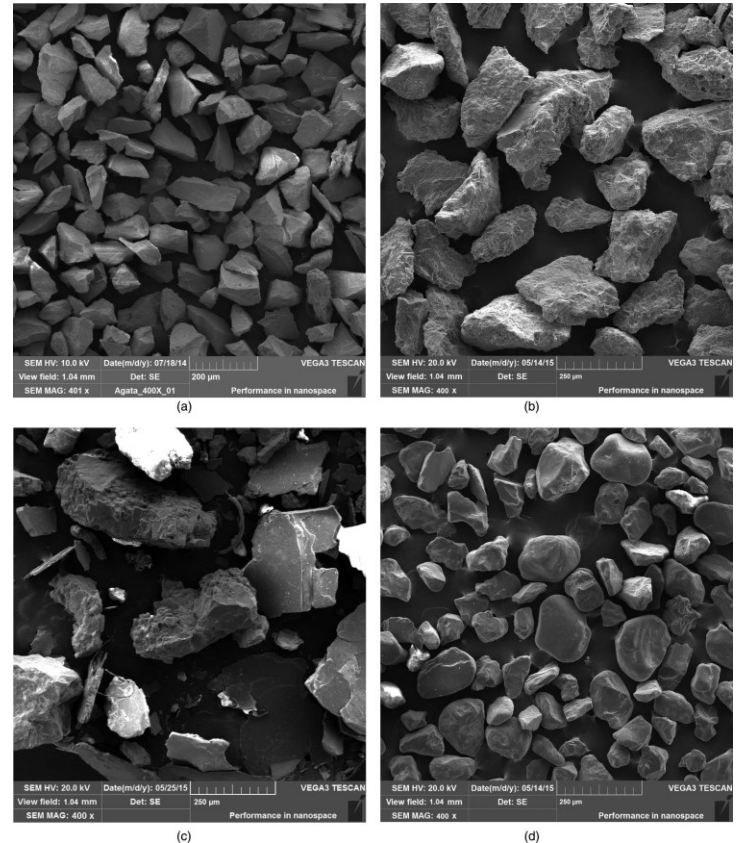


Triaxial results on sand-cement blends: unique deviatoric stress - axial strain curve

(unique η/C_{iv} but triaxial tests with distincts cement contents and distinct porosities)

Sand-Cement Dosage (Clean Sands)

Shapes of studied sands using a scanning electron microscope (SEM): (a) angular silica sand obtained as a by-product of agate polishment; (b) rough sand made from crushed basalt; (c) granitic Porto sand; (d) rounded Osorio sand

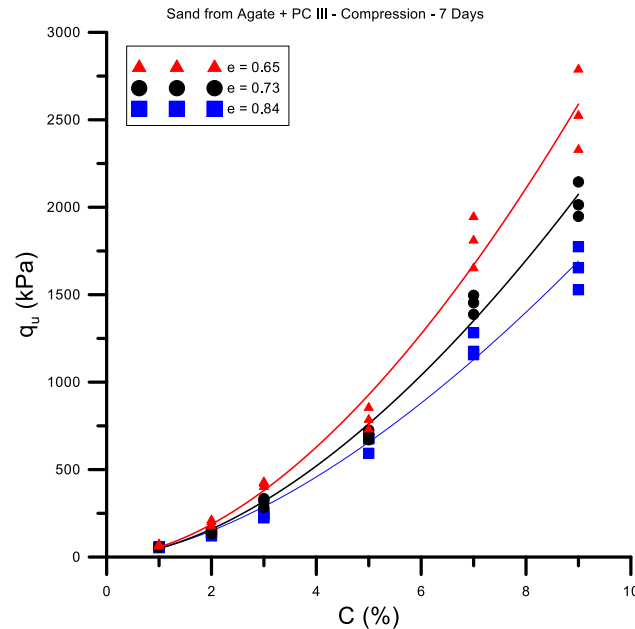


Consoli et al. (2017).

“Broad-spectrum empirical correlation determining tensile and compressive strength of cement-bonded clean granular soils”.

Journal of Materials in Civil Engineering 29 (6), 06017004

Sand-Cement Dosage (Clean Sands)



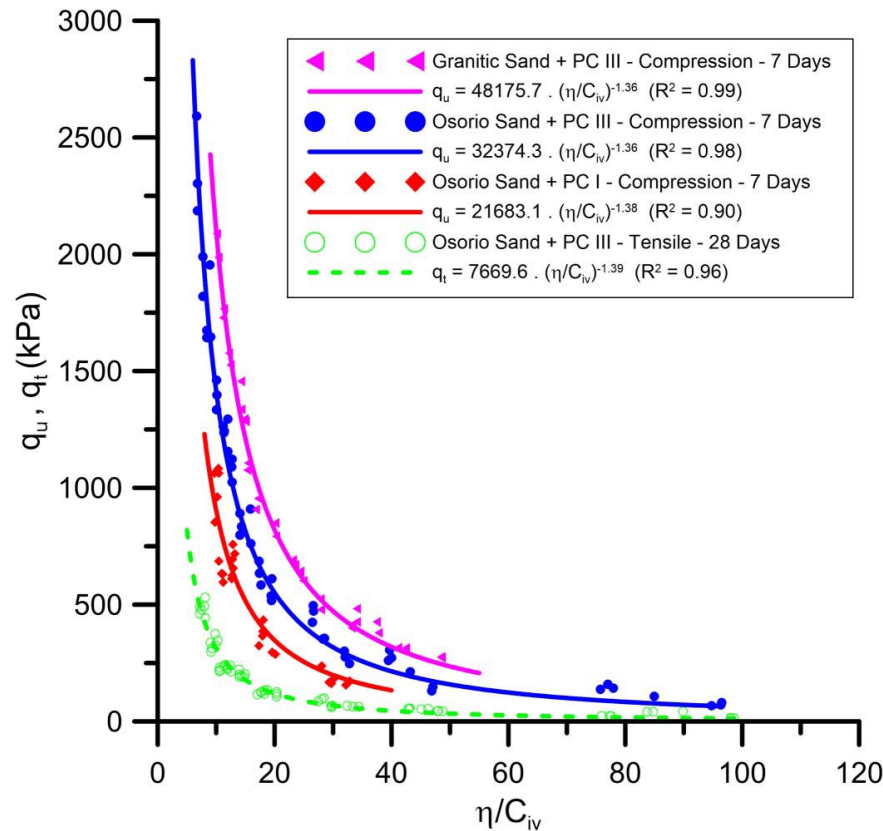
Unconfined compressive strength (q_u) of silica sand obtained as a by-product of agate polishment treated with early strength Portland cement content for three distinct void ratio and 7 days as curing period.

Consoli et al. (2017).

“Broad-spectrum empirical correlation determining tensile and compressive strength of cement-bonded clean granular soils”.

Journal of Materials in Civil Engineering, 29 (6), 06017004

Sand-Cement Dosage (Clean Sands)



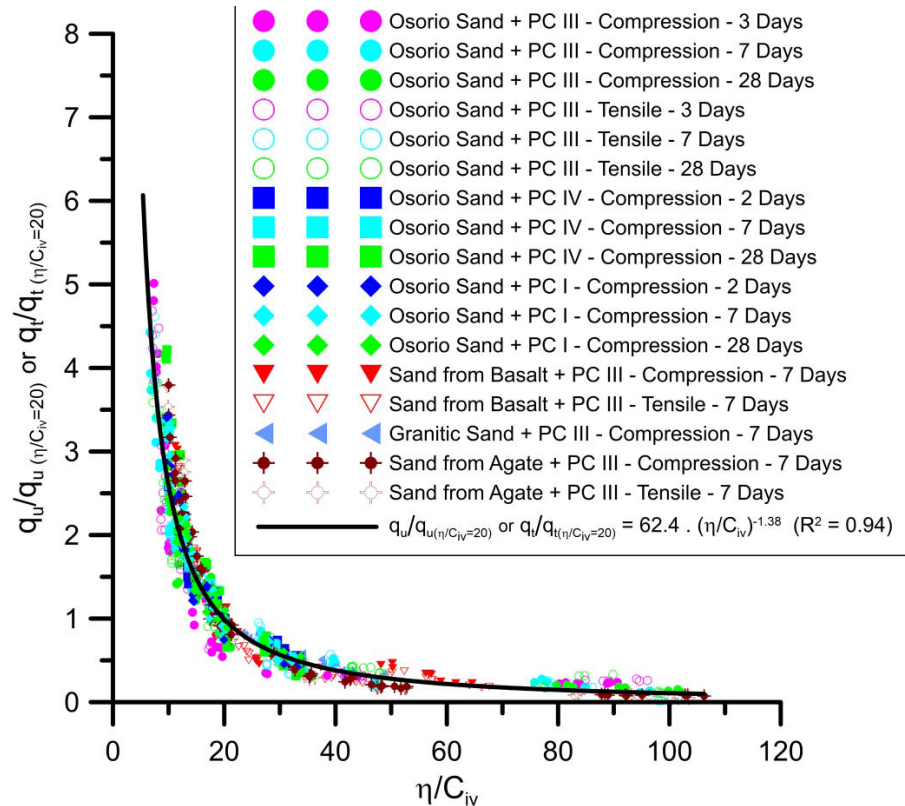
Examples of best-fit curves of q_u (or q_t) versus η/C_{iv} for studied sands treated with Portland cement

Consoli et al. (2017).

“Broad-spectrum empirical correlation determining tensile and compressive strength of cement-bonded clean granular soils”.

Journal of Materials in Civil Engineering, 29 (6), 06017004

Sand-Cement Dosage (Clean Sands)



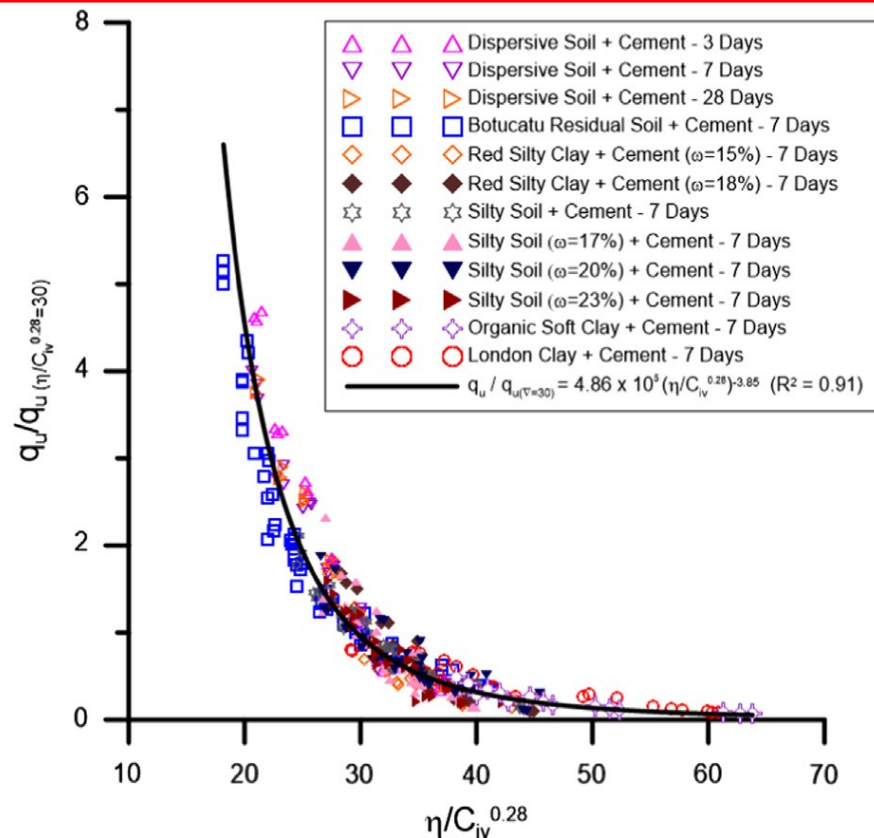
Normalization of q_u or q_t (for the whole range of η/C_{iv}) by dividing for q_u or q_t at $\eta/C_{iv} = 20$, considering distinct Portland cement types under curing times from 2 to 28 days.

Consoli et al. (2017).

“Broad-spectrum empirical correlation determining tensile and compressive strength of cement-bonded clean granular soils”.

Journal of Materials in Civil Engineering 29 (6), 06017004

Fine-Grained Soil-Cement Dosage



Normalisation of q_u (for the whole range of $\eta/C_{iv}^{0.28}$) with adjusted porosity/cement index for all fine-grained soils studied and considering distinct curing periods (3, 7 and 28 days).

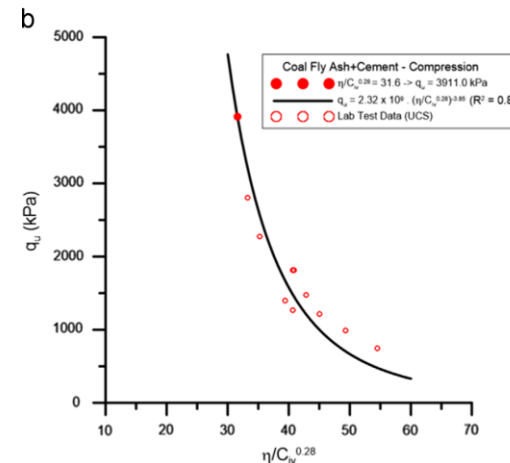
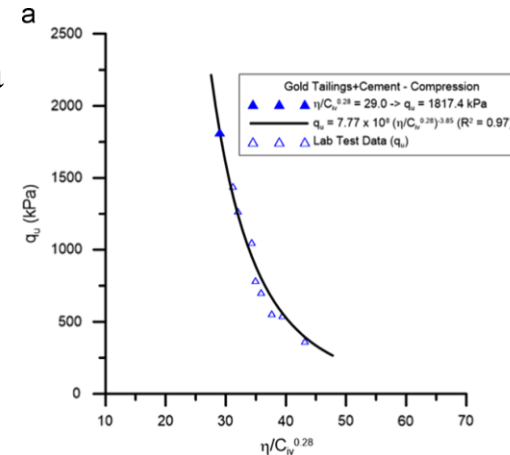
Consoli et al. (2016)

“A unique relationship determining strength of silty/clayey soils-Portland cement mixes”.
Soils and Foundations, 56 (6), 1082-1088.

Fine-Grained Soil-Cement Dosage

Curve obtained using Eq. (7) and lab-testing data for (a) gold tailings - Portland cement and (b) coal fly ash-Portland cement.

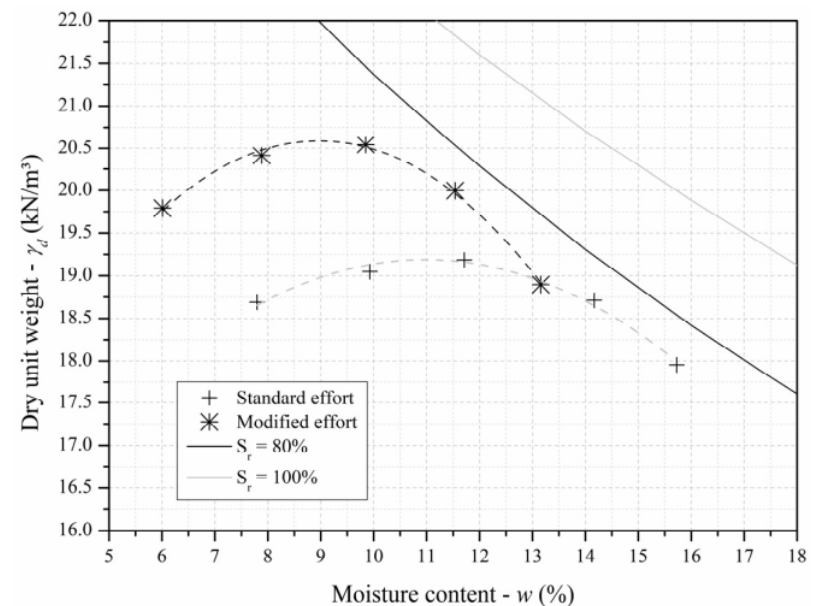
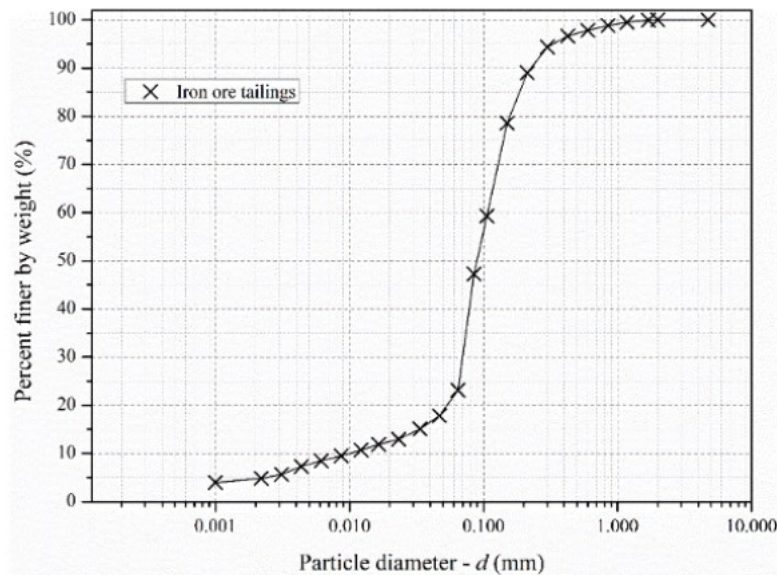
$$\frac{q_u}{q_u \text{ (for particular } \nabla = 30)} = 486,000 \left[\frac{\eta}{(C_{iv})^{0.28}} \right]^{-3.85}$$



Consoli et al. (2016)

“A unique relationship determining strength of silty/clayey soils-Portland cement mixes”.
Soils and Foundations, 56(6), 1082-1088.

Compacted filtered iron ore tailings–Portland cement blends

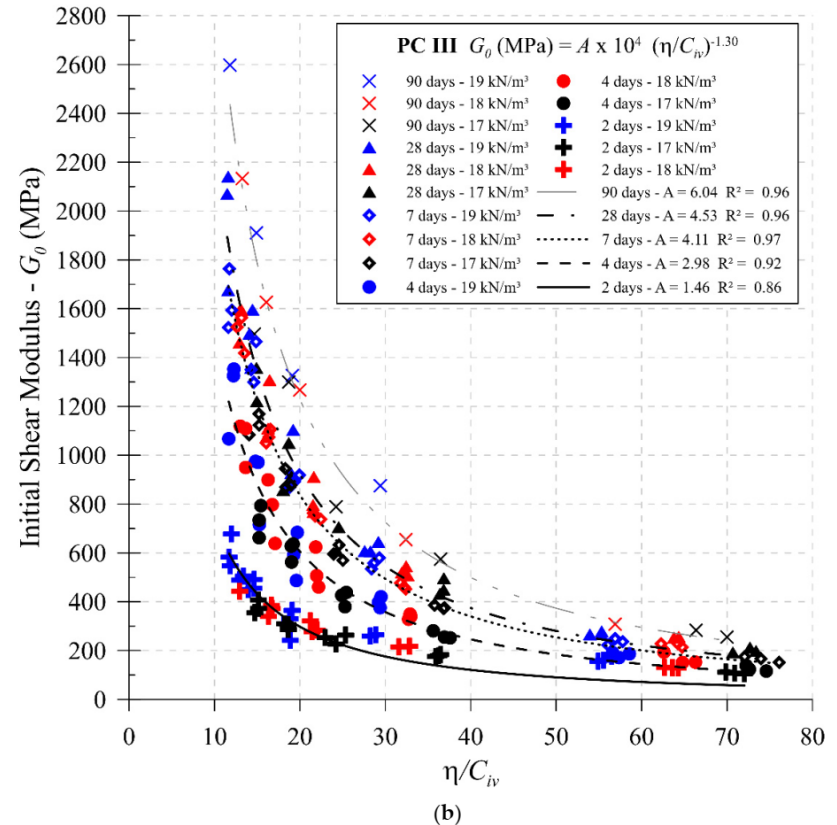
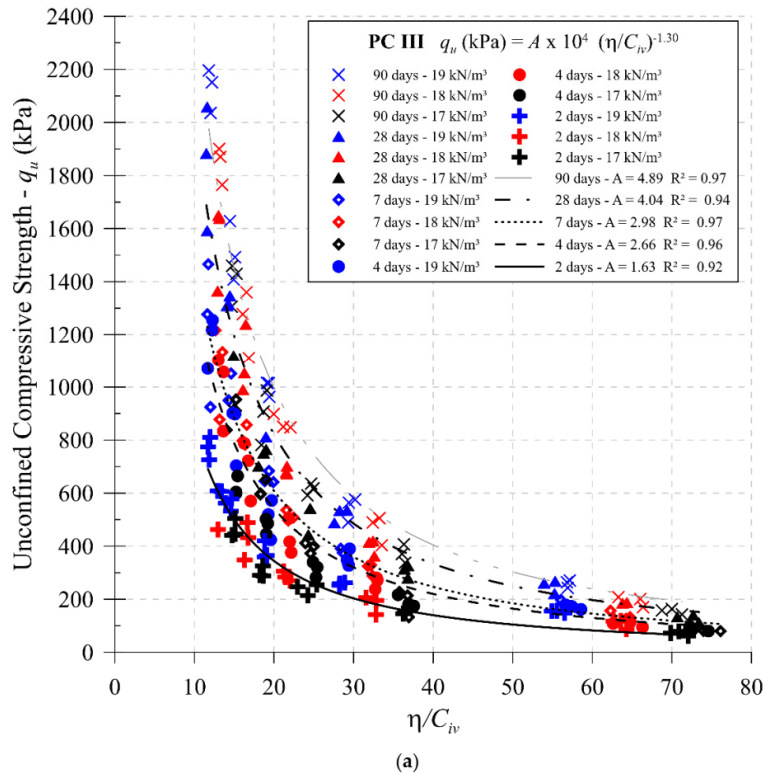


CONSOLI, N. C.; VOGT, J. C.; SILVA, J. P.; CHAVES, H. M.; SCHEUERMANN FILHO, H. C.; MOREIRA, E. B.; LOTERO, A. (2022).

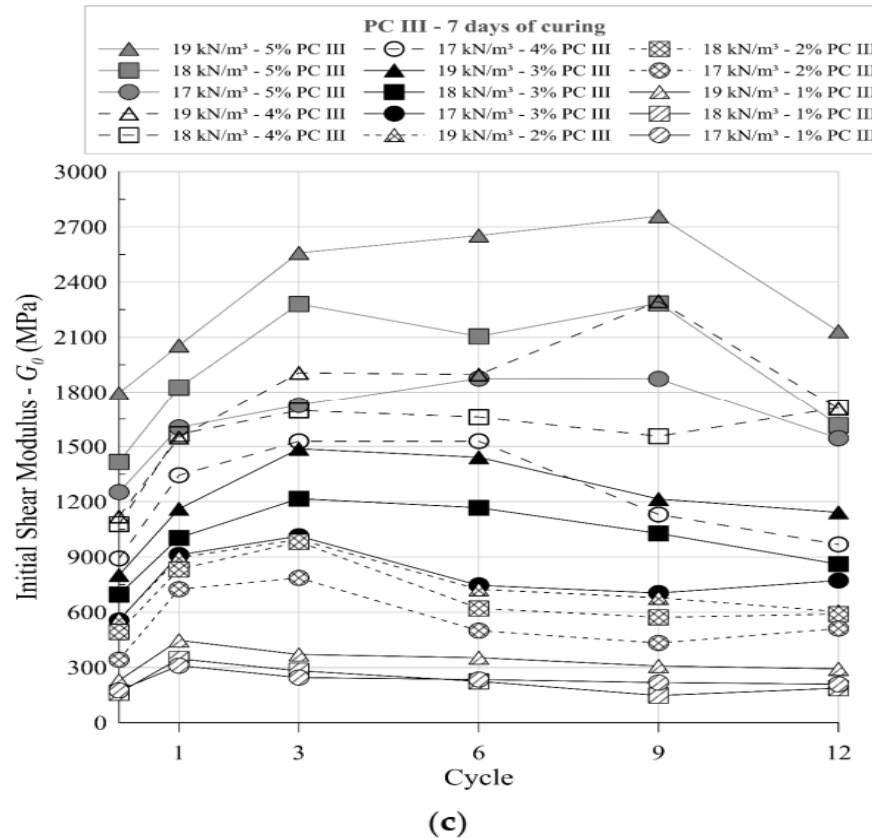
Behaviour of compacted filtered iron ore tailings–Portland cement blends: New Brazilian trend for tailings disposal by stacking.

Applied Sciences, 12, 836 (DOI: 10.3390/app12020836).

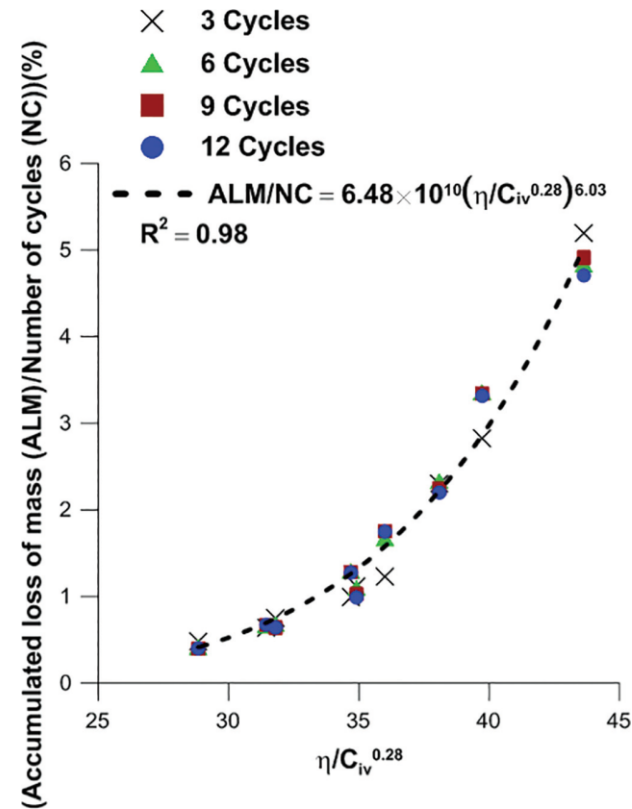
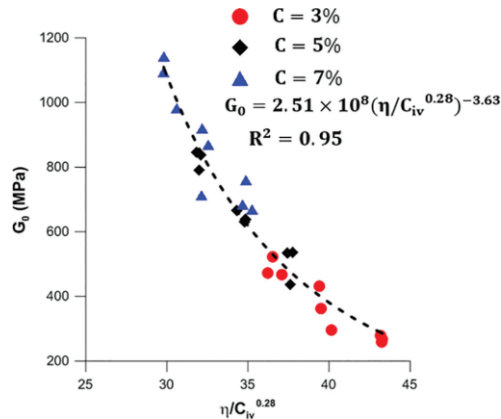
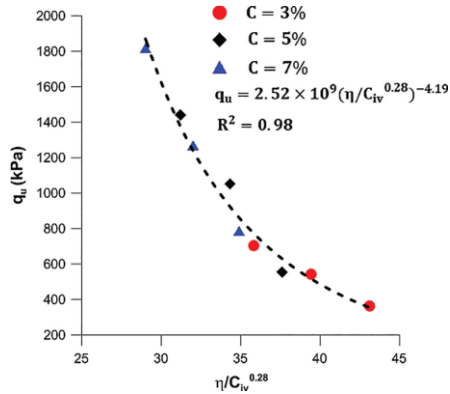
Compacted filtered iron ore tailings–Portland cement blends



Compacted filtered iron ore tailings–Portland cement blends

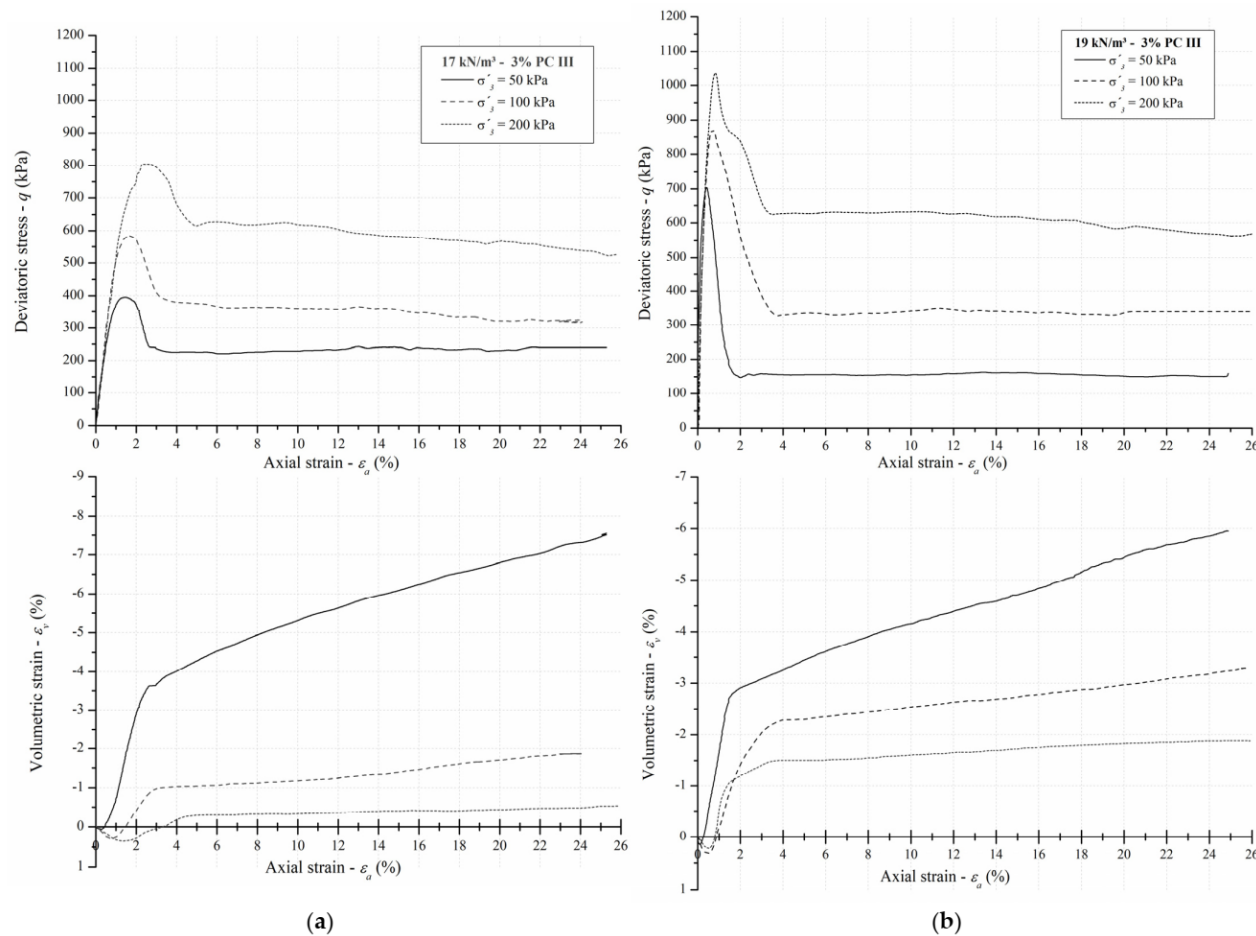


Durability, strength, and stiffness of compacted gold tailings – cement mixes

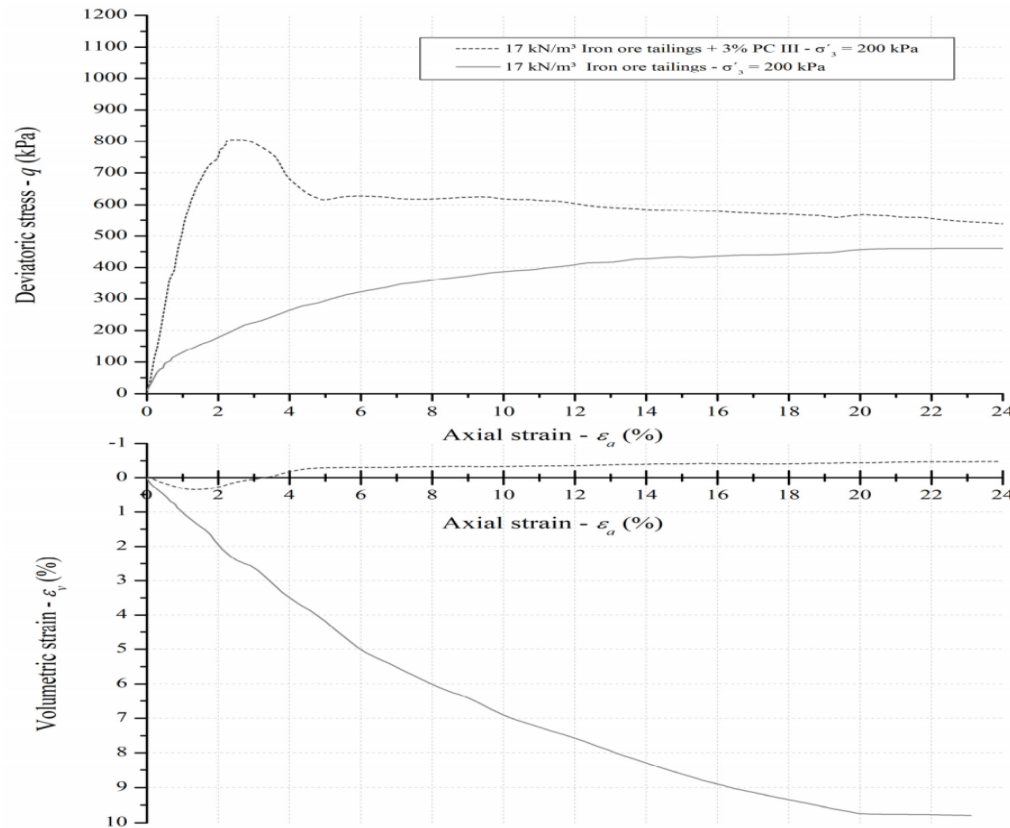


Consoli, N. C., Peccin, A., Sosnoski, J., Nierwinski, H. P. (2018)
 “Durability, strength, and stiffness of compacted gold tailings – cement mixes”.
Canadian Geotechnical Journal, 55(6), 486-494.

Compacted filtered iron ore tailings–Portland cement blends



Compacted filtered iron ore tailings–Portland cement blends

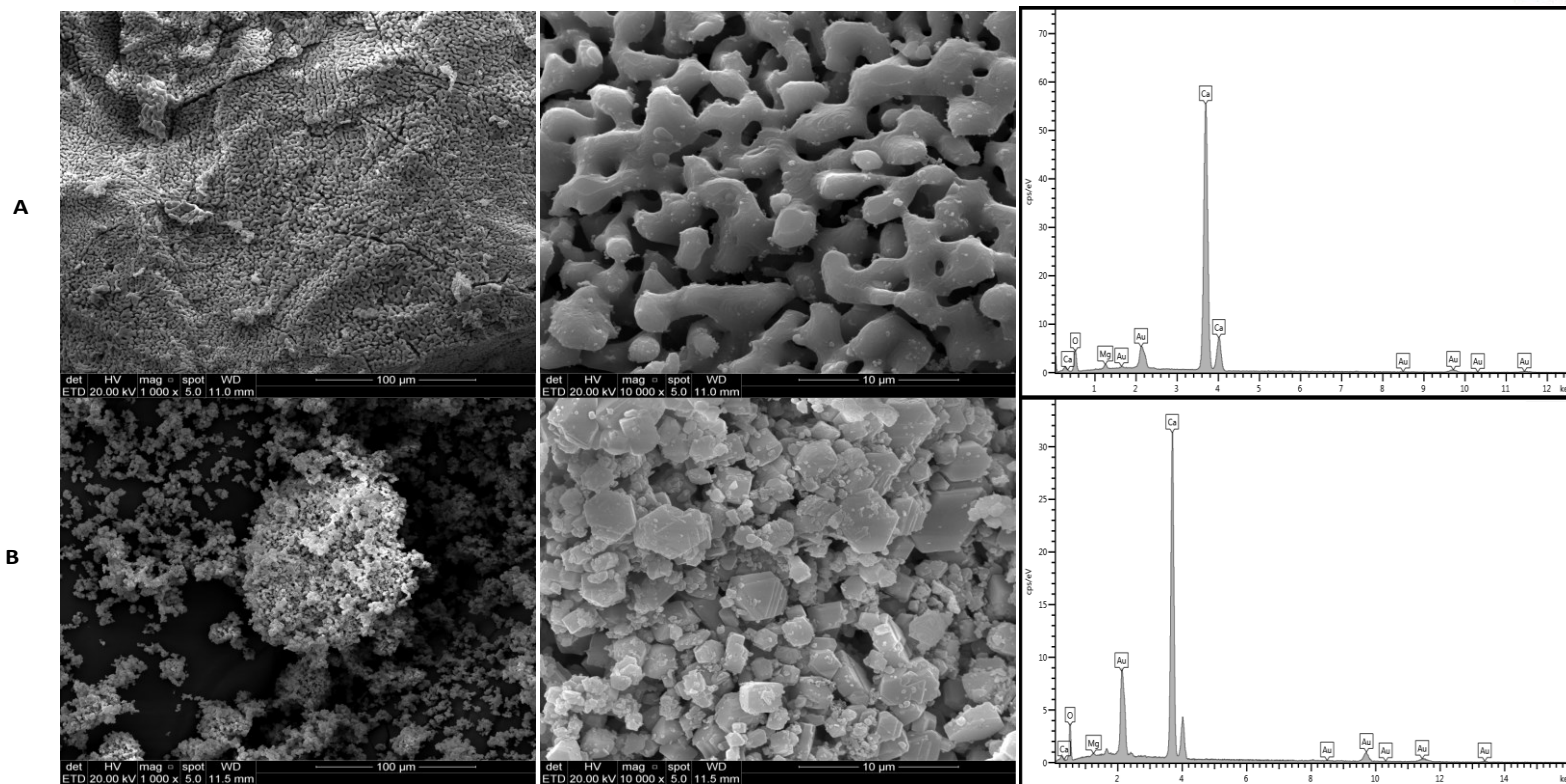


**Alternative (sustainable)
cements for filtered
compacted cemented dry
stacking (300 m high)**

Research lines related to Sustainability

- Use of industrial, agricultural, domestic and construction wastes in the improvement of geomaterials (including tailings);
- Development of new alternatives for earthwork solutions that minimize environmental impacts, and are more economical and maximize social welfare;
- Environmental, economic, and social life cycle analysis for determining sustainable solutions.

Scanning electron microscopy with EDS spectrogram for (a) quicklime and (b) hydrated lime from eggshell.



Consoli, N. C.; Lotero, A.; Saldanha, R. B.; Scheuermann Filho, H. C.; Moncaleano, C. (2020).
 “Eggshell produced limes: Innovative materials for soil stabilization.”
Journal of Materials in Civil Engineering, 32(11), 06020018.

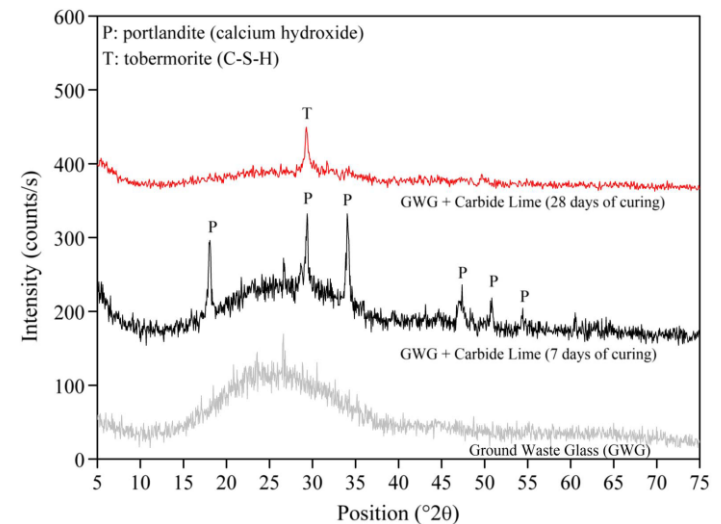
QUICKLIME and HYDRATED LIME from
EGGSHELL

+

GROUND GLASS

=

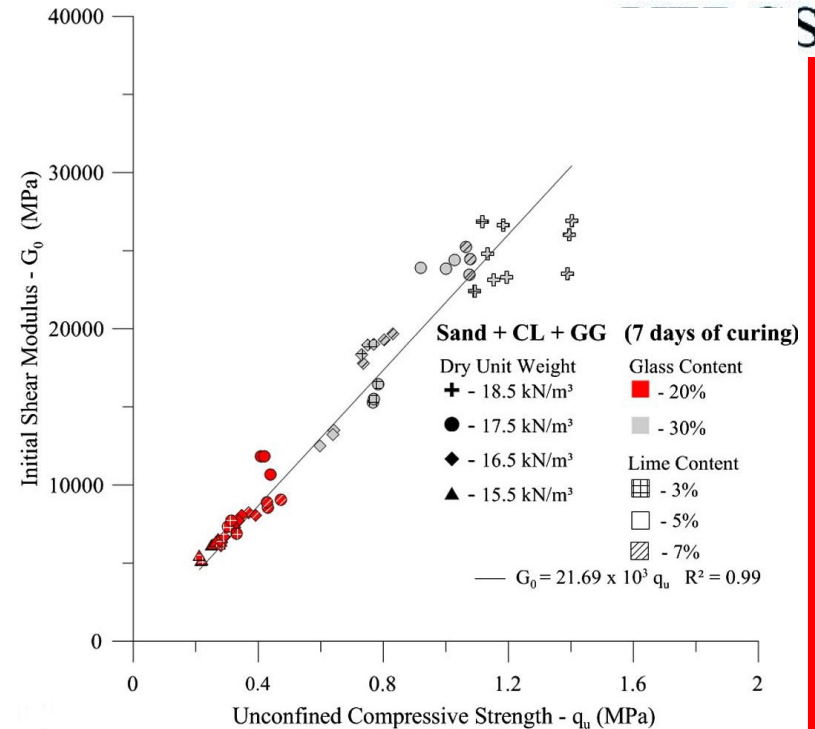
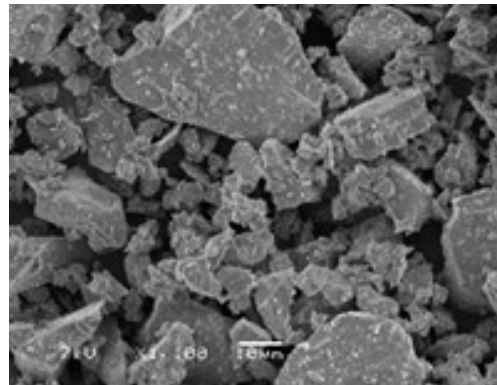
New Binder



X-ray diffractometry of ground glass, lime and blend of both

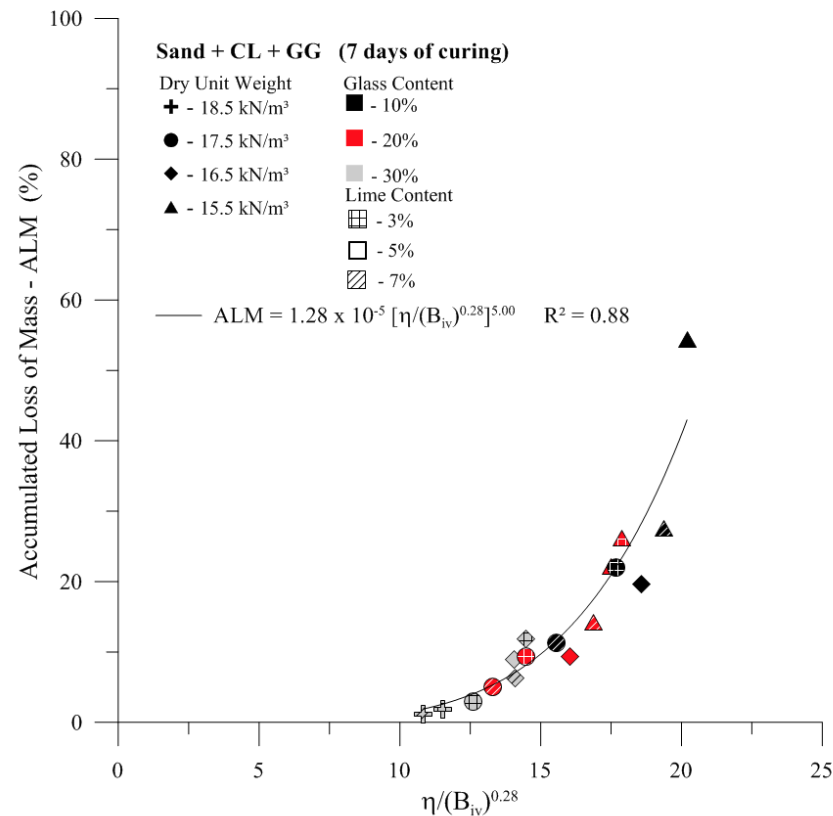
Patent of a new binder

PÓS
ENG



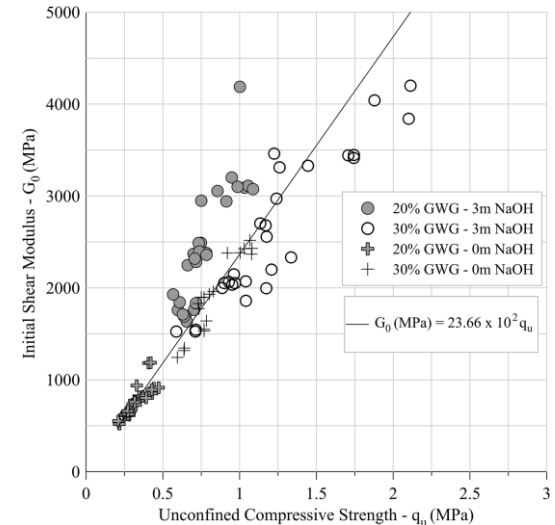
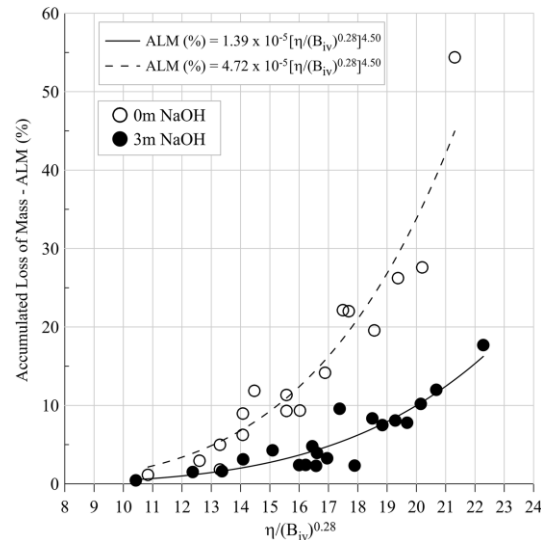
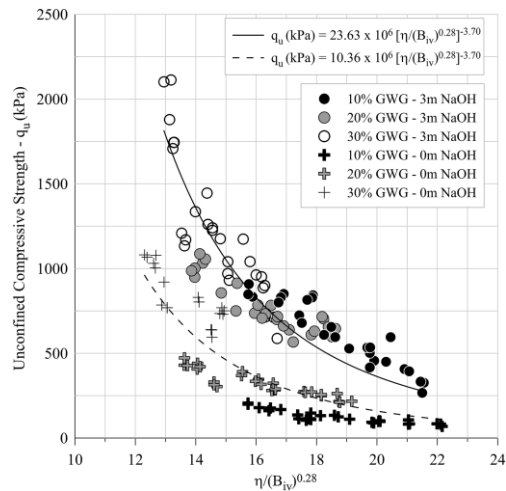
Unconfined compressive strength (q_u) versus initial shear stiffness (G_0) for sand–ground glass–carbide lime compacted blends considering 20 and 30% of ground glass; 3, 5 and 7% of carbide lime; and the studied dry unit weights considering 7 days of curing.

Durability, strength and stiffness of green stabilized sand



Consoli, N. C. et al. (2021).
 “Ground waste glass–carbide lime as a sustainable binder stabilising three different silica sands.”
Géotechnique, 71(6), 480-493.

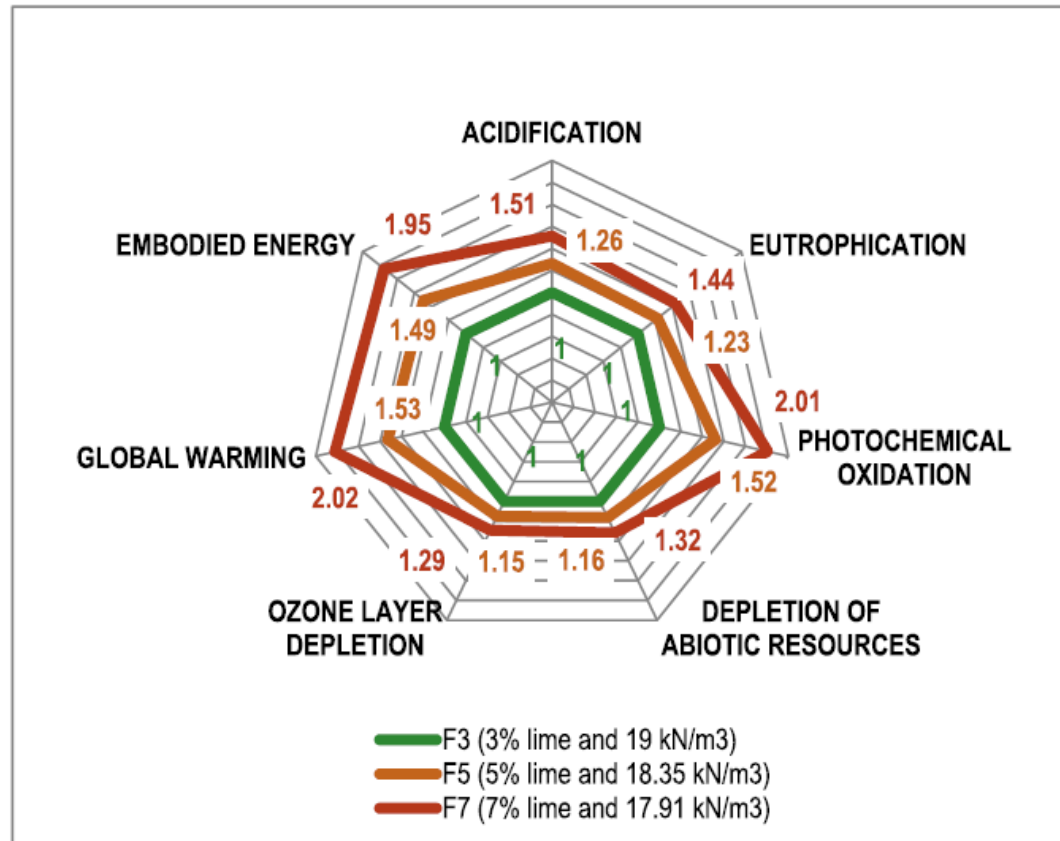
Lime-ground glass-sodium hydroxide as an enhanced sustainable binder stabilizing silica sand



Consoli, N. C.; Daassi-Gli, C. P. A. et al. (2021).

“Lime-ground glass-sodium hydroxide as an enhanced sustainable binder stabilizing silica sand.”

Journal of Geotechnical and Geoenvironmental Engineering, 147(10), 06021011.



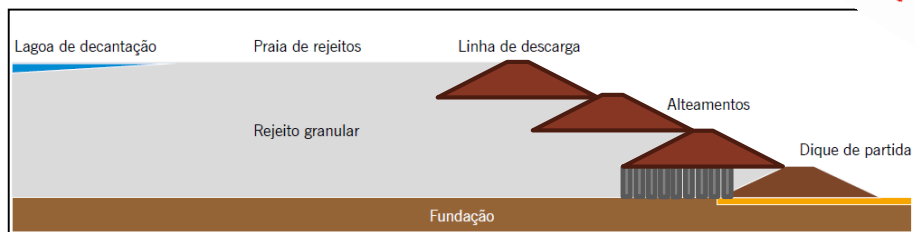
**TAILINGS *IN SITU*
IMPROVEMENT USING
BINDERS
(for safe decommissioning)**

TAILINGS *IN SITU* IMPROVEMENT USING BINDERS (for safe decommissioning)

Upstream dam tailings improvement through deep mixing

POSSIBLE MITIGATION ALTERNATIVES

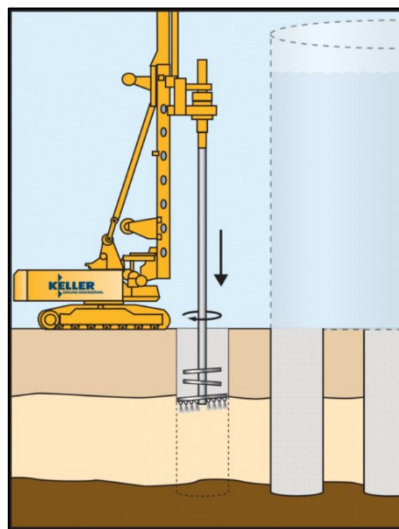
(for upstream dams)



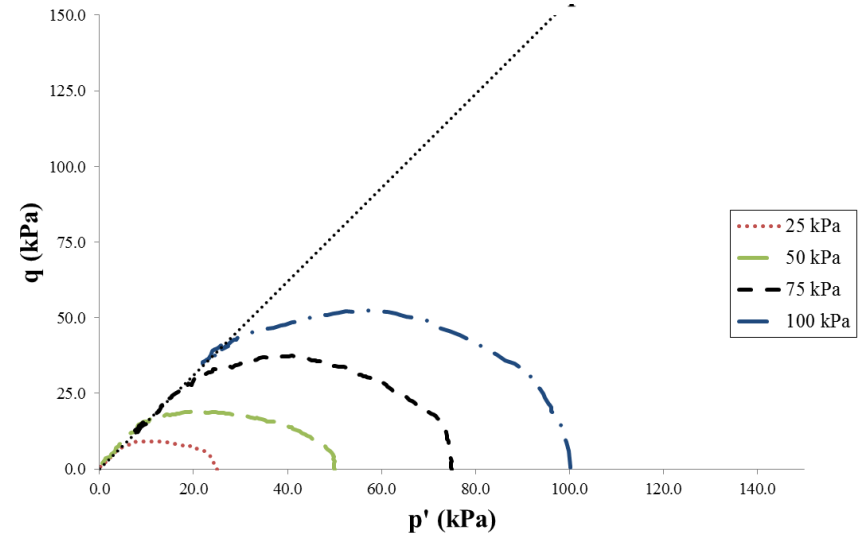
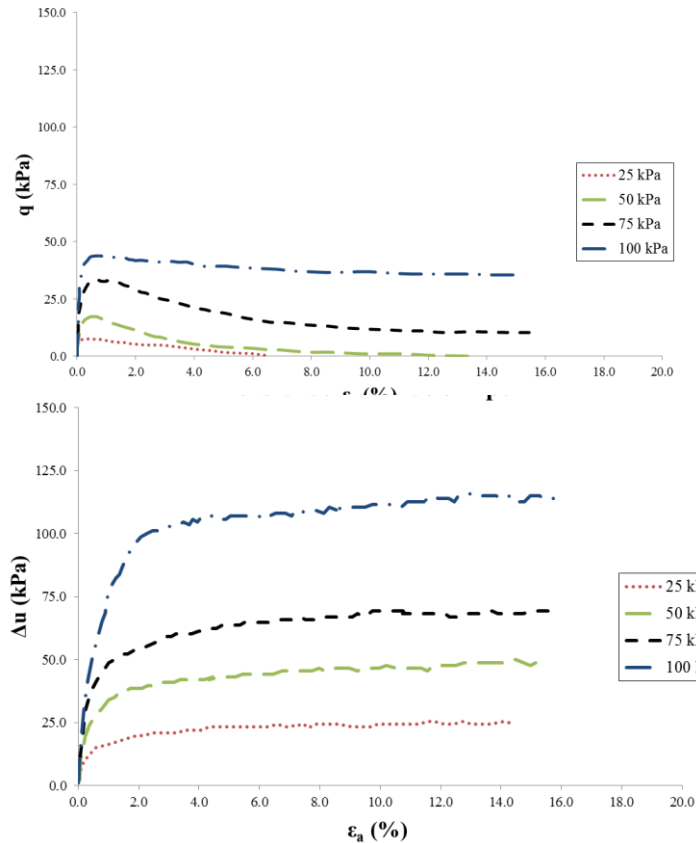
GROUND IMPROVEMENT TECHNIQUES

DEEP SOIL MIXING (DSM)

Addition of cementing agents that are mechanically mixed with the site soil, producing columns of improved soil.



- MITIGATION OF LIQUEFACTION POTENTIAL;
- INCREASED STABILITY;
- FLOW CONTROL (BARRIER FUNCTION).



Consoli, N.C.; Tomasi, L. F.; Marques, S. (2023)

“Cement enhancing mechanical behavior of tailings behind upstream tailings dam for safe decommissioning”

Journal of Materials in Civil Engineering, ASCE (DOI: 10.1061/(ASCE)MT.1943-5533.0004741)

Cement enhancing mechanical behavior of tailings *in situ*

Gold tailings with high void ratio of about 1.10 and high moisture content (same as found in the field) mixed with Portland cement



Gold tailings with high void ratio of 1.10 and high moisture content of about 40%, mixed with Portland cement

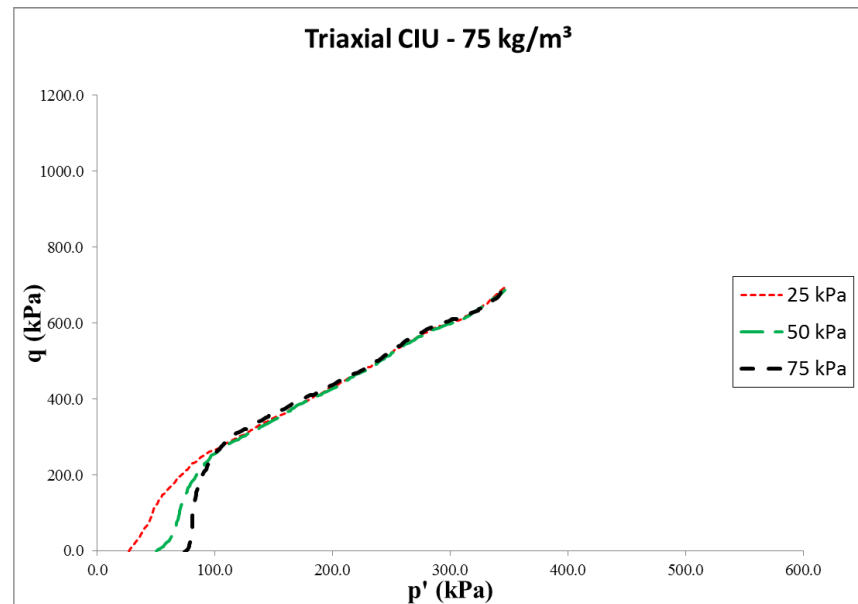
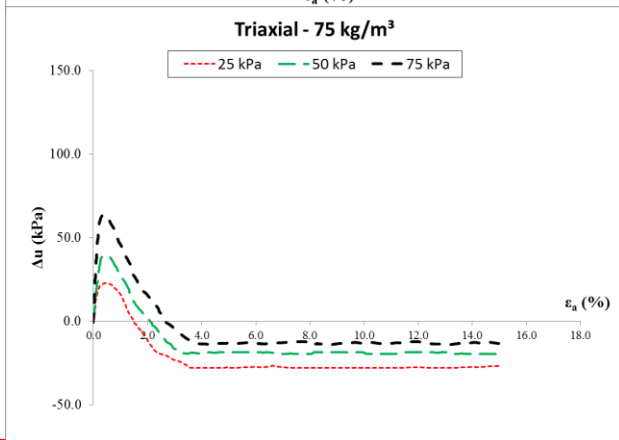
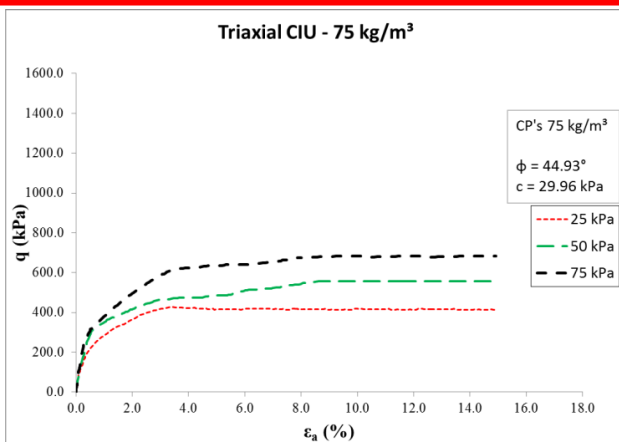


Specimens of gold tailings - Portland cement
gold tailings blends

Consoli, N.C.; Tomasi, L. F.; Marques, S. (2023)

“Cement enhancing mechanical behavior of tailings behind upstream tailings dam for safe decommissioning ”
Journal of Materials in Civil Engineering, ASCE (DOI: 10.1061/(ASCE)MT.1943-5533.0004741)

Cement enhancing mechanical behavior of tailings *in situ*

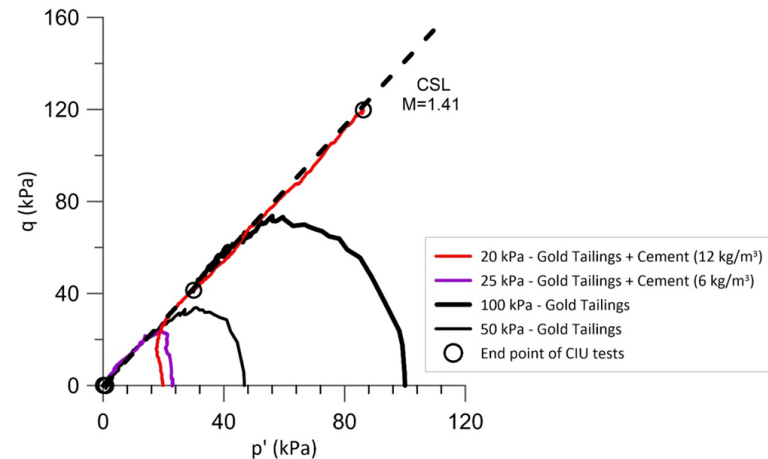
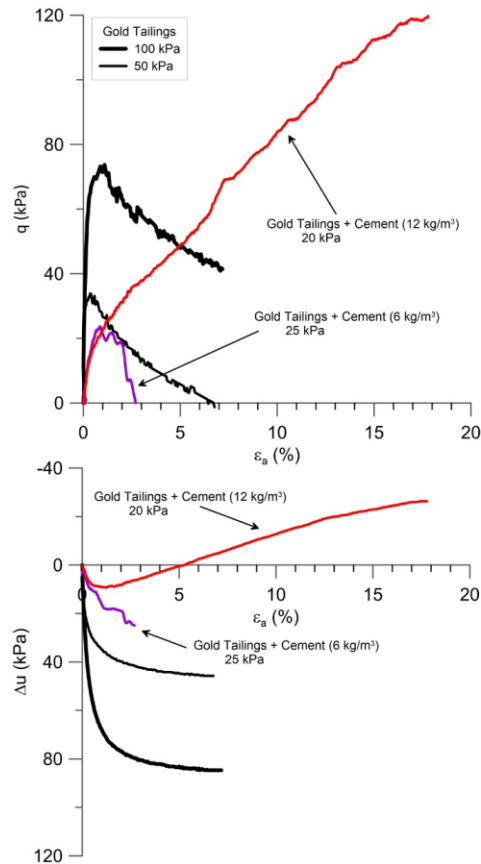


Consoli, N.C.; Tomasi, L. F.; Marques, S. (2023)

“Cement enhancing mechanical behavior of tailings behind upstream tailings dam for safe decommissioning”

Journal of Materials in Civil Engineering, ASCE (DOI: 10.1061/(ASCE)MT.1943-5533.0004741)

Cement enhancing mechanical behavior of tailings *in situ*



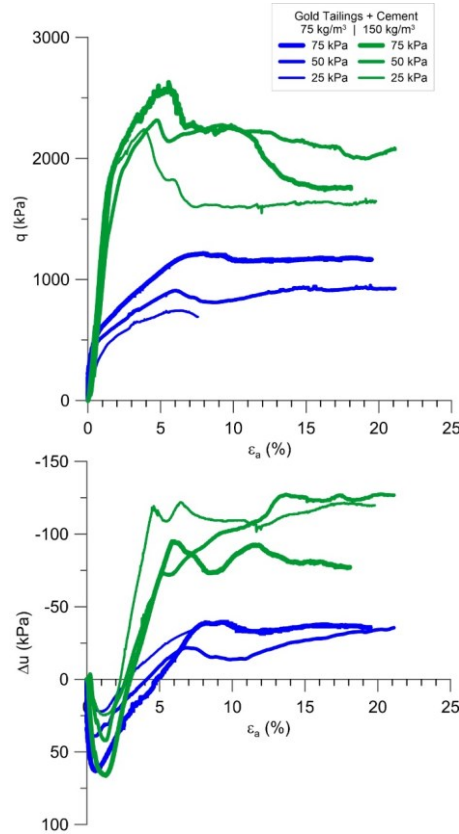
Stress paths of reconstituted gold tailings under undrained triaxial tests, as well as slight (6 and 12 kg/m³) amounts of Portland cement gold tailings

Consoli, N.C.; Tomasi, L. F.; Marques, S. (2023)

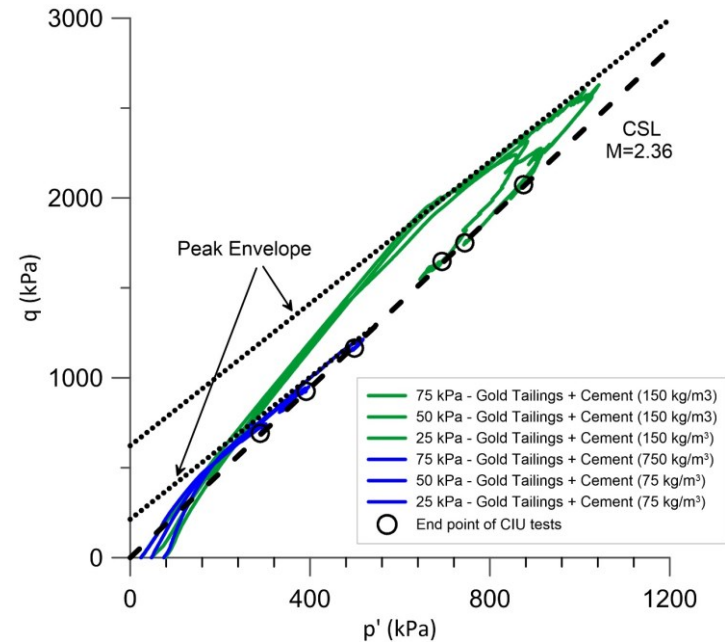
“Cement enhancing mechanical behavior of tailings behind upstream tailings dam for safe decommissioning ”

Journal of Materials in Civil Engineering, ASCE (DOI: 10.1061/(ASCE)MT.1943-5533.0004741)

Cement enhancing mechanical behavior of tailings *in situ*



Stress-strain-pore-pressure curves for the undrained triaxial tests on substantial amounts (75 kg/m³ and 150 kg/m³) of Portland cement gold tailings

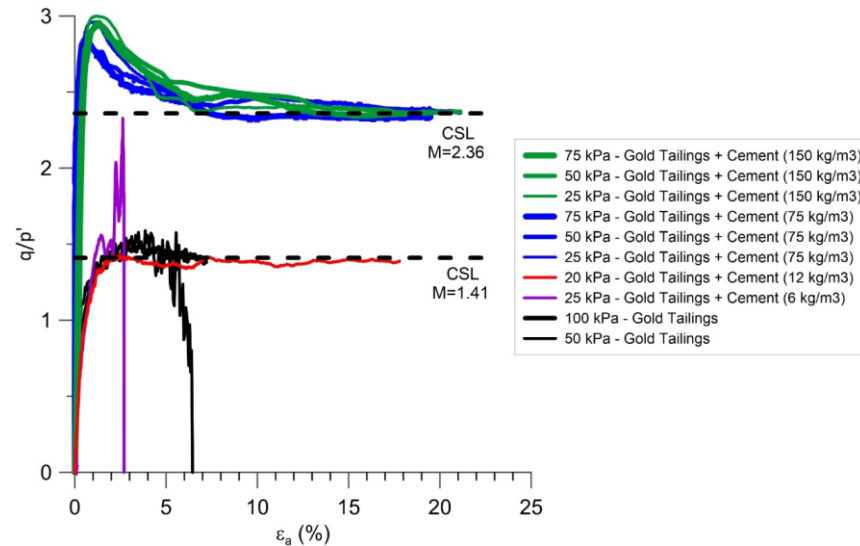


Stress paths of undrained triaxial tests of substantial amounts of Portland cement gold tailings

Consoli, N.C.; Tomasi, L. F.; Marques, S. (2023)

“Cement enhancing mechanical behavior of tailings behind upstream tailings dam for safe decommissioning ”
Journal of Materials in Civil Engineering, ASCE (DOI: 10.1061/(ASCE)MT.1943-5533.0004741)

Cement enhancing mechanical behavior of tailings *in situ*



Stress ratio (q/p') versus axial strain (ϵ_a) plot

Consoli, N.C.; Tomasi, L. F.; Marques, S. (2023)

“Cement enhancing mechanical behavior of tailings behind upstream tailings dam for safe decommissioning ”

Journal of Materials in Civil Engineering, ASCE (DOI: 10.1061/(ASCE)MT.1943-5533.0004741)



Thank you!

Knowledge

Let it flower

It will shape your future